

DETECTION OF CALIX[6]ARENE POLYMERIZATION  
USING FOURIER TRANSFORM INFRARED SPECTROSCOPY

THESIS

Presented to the Graduate Council  
of Texas State University-San Marcos  
in Partial Fulfillment  
of the Requirements

for the Degree

Master of SCIENCE

by

Matthew Josiah McDougale

San Marcos, Texas  
May 2008

**COPYRIGHT**

**by**

**Matthew Josiah McDougale**

**2008**

## ACKNOWLEDGEMENTS

I would first like to thank my family for their support throughout my time in school. Their words of inspiration have aided me in my journey and have guided me through many of the tough times.

I would like to express my gratitude to Dr. David Donnelly for his patience and understanding during my thesis studies. His professionalism throughout my time at Texas State University-San Marcos inspired me to be a better student in physics as well as a student of life. He, along with the other members of my thesis committee, Dr. Geerts and Dr. Golding, supported me in my efforts and for that I am truly grateful. As a long time student here at Texas State I have enjoyed my time here and to that I owe the entire Physics Department. I have received a fine education here and feel that because of their efforts, I will be prepared for the next step of my life.

I would like to thank all of my friends who have supported me in their own way throughout my studies. While none of them had to do the work, they all were forthcoming with words of advice or motivation.

Finally, I would like to thank the others who have contributed to my work here. Nelson Koeck has been a great support with respect to ensuring I had the complimentary supplies needed for my thesis. Dr. Spencer and Dr. Blanda were always available for questions when I had them.

This manuscript was submitted on April 28, 2008

## TABLE OF CONTENTS

	Page
ACKNOWLEDGEMENTS .....	iv
LIST OF FIGURES.....	viii
LIST OF SPECTRA.....	x
LIST OF TABLES.....	xii
CHAPTERS	
1 INTRODUCTION .....	1
1.1 Lithography .....	3
2 CHEMISTRY OF CALIX[6]ARENES.....	7
3 FOURIER TRANSFORM INFRARED SPECTROSCOPY .....	14
3.1 Theory of Infrared Absorption .....	14
3.2 Theory of FTIR.....	21
4 EXPERIMENT AND RESULTS .....	30
4.1 Calix[6]arene Preparation .....	30
4.2 Calix[6]arene Deposition.....	30
4.3 UV Exposure of Calix[6]arenes .....	32
4.4 FTIR Analysis.....	32
4.5 IR Spectra .....	37
5 CONCLUSION .....	59

Appendix .....	62
Bibliography .....	71

## List of Figures

Figure	Page
1.1: Moore's Law.....	2
2.1: Benzene Ring.....	7
2.2: Hexyl Groups .....	8
2.3: Xylenyl Groups.....	8
2.4: Cone and 1,2,3 Alternate Conformation .....	9
2.5: Shorthand and Structural Representation of Allyl Groups .....	9
2.6(a-j): Ten Calix[6]arene Molecules .....	10-11
2.6a: OC Calix[6]arene .....	10
2.6b: 2C Calix[6]arene .....	10
2.6c: 4C Calix[6]arene .....	10
2.6d: 6C Calix[6]arene .....	10
2.6e: 8C Calix[6]arene .....	10
2.6f: OA Calix[6]arene .....	10
2.6g: 2A Calix[6]arene .....	11
2.6h: 4A Calix[6]arene .....	11
2.6i: 6A Calix[6]arene .....	11
2.6j: 8A Calix[6]arene .....	11

2.7: Cross Linking of Allyl Groups .....	12
3.1: Absorptions of Radiation by Molecules .....	15
3.2: Molecular Energy Reactions and IR Molecular Vibrational Variations.....	16
3.3: C=C and C-C Stretching Regions of an IR Spectrum.....	20
3.4: Michelson Interferometer.....	21
4.1: Wafer Spinner .....	31
4.2: Interferogram and the MCT Detector.....	34
4.3: Background Spectrum with and without Si .....	35
4.4: Subtracted Spectrum Test.....	36
4.5: C=C and C-C stretching regions of an IR spectra .....	38
4.6: Cross Linking of Allyl Groups .....	39
4.7: Benzene Absorbance Spectra.....	43
A.1: Checking the Dessicant .....	64
A.2: Experiment Setup Window.....	65
A.3: Signal to Noise Improvement.....	65
A.4: Optimal Beamsplitter-Detector Combinations .....	67
A.5: Screen Type Versus Transmitted Radiation.....	68
A.6: Bench Tab of Experiment Setup Tab .....	69

## List of Spectra

2A	Page
Spectrum 4.1: Unexposed.....	40
Spectrum 4.2: 2 minute exposure.....	40
Spectrum 4.3: 5 minute exposure.....	41
Spectrum 4.4: 10 minute exposure.....	41
Spectrum 4.5: 20 minute exposure.....	42
Spectrum 4.6: 1000 minute exposure.....	42
8A	
Spectrum 4.7: Unexposed.....	44
Spectrum 4.8: 2 minute exposure.....	45
Spectrum 4.9: 5 minute exposure.....	45
Spectrum 4.10: 10 minute exposure.....	46
Spectrum 4.11: 20 minute exposure.....	46
Spectrum 4.12: 1000 minute exposure.....	47
2C	
Spectrum 4.13: Unexposed.....	48
Spectrum 4.14: 2 minute exposure.....	49
Spectrum 4.15: 5 minute Exposure.....	49

Spectrum 4.16: 10 minute exposure.....	50
Spectrum 4.17: 20 minute exposure.....	50
Spectrum 4.18: 1000 minute exposure.....	51

## 8C

Spectrum 4.19: Unexposed.....	52
Spectrum 4.20: 2 minute exposure.....	52
Spectrum 4.21: 5 minute exposure.....	53
Spectrum 4.22: 10 minute exposure.....	53
Spectrum 4.23: 20 minute exposure.....	54
Spectrum 4.24: 1000 minute exposure.....	54

## 8C with Si and OC in the Background

Spectrum 4.25: Unexposed.....	55
Spectrum 4.26: 2 minute exposure.....	56
Spectrum 4.27: 5 minute exposure.....	56
Spectrum 4.28: 10 minute exposure.....	57
Spectrum 4.29: 20 minute exposure.....	57
Spectrum 4.30: 1000 minute exposure.....	58

## List of Tables

Table 1.1:	Gate dimension projections as reported by the ITRS - 2007 edition.....	3
Table 3.1:	IR Absorption Regions of Basic Bond Structures.....	20

# CHAPTER 1

## INTRODUCTION

The trend of the modern IC is, as it has always been, to become smaller and smaller. With this miniaturization of devices comes the necessity for improvement of current methodologies as well as innovations to surpass barriers encountered when trying to shrink devices to the next level, whilst still maintaining or improving current device performance. Many factors must be considered and while some device performance keystones are improved with the miniaturization of devices - power requirements, information per area on chip, and processing speed to name a few - the real challenge is finding methods to achieve the next steps of miniaturization.

One common device, the transistor, has been scaled down since the beginning of its creation. Its purpose is to serve as a data point storage device and is programmed to either contain charge or not contain charge. This is the basis of all information storage as computers are programmed to read the presence or lack of charge as a 1 or a 0 (binary). The earlier transistors were large and only a few could be integrated into a circuit which meant that little information could be stored. Today this is not the case. So how does one make devices smaller? The reduction of feature size is the benchmark of miniaturization. Recalling the transistor, we can see that the smaller a device is,

the larger the quantity per unit area. Scaling of these devices has been regulated/motivated since the mid 90's by the The International Technology Roadmap for Semiconductors (ITRS). The ITRS forecasts the goals and hurdles of feature size scaling 15 years in advance. This foresight has benefitted the industry and has kept the trend of miniaturization on a course roughly in tune with Gordon Moore's Law up to the present (Figure 1.1).

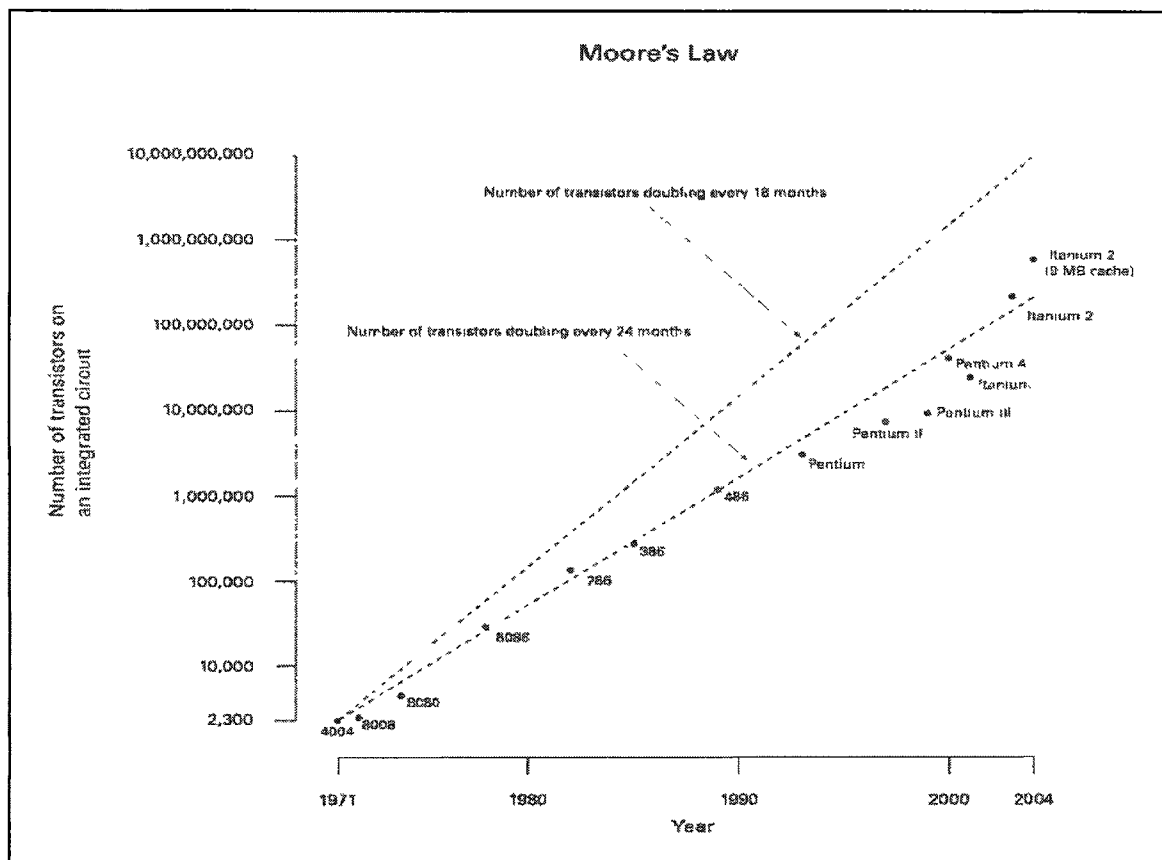


*Figure 1.1: Moore's Law: Gordon Moore predicted the trend that the number of transistors on an integrated circuit would double every two years. As can be seen, this trend has been maintained with minimal deviation<sup>1</sup>.*

Today, The ITRS reports that feature sizes of transistors are 65 nm and by 2010 they are predicted to reach 50nm<sup>2</sup> (Table 1.2). Until recently, this trend has been relatively manageable, but the devices are now approaching limits of scaling due

*Table 1.1: Gate dimension projections as reported by the ITRS - 2007 edition<sup>2</sup>*

<i>Year of Production</i>	<i>2007</i>	<i>2008</i>	<i>2009</i>	<i>2010</i>	<i>2011</i>	<i>2012</i>	<i>2013</i>	<i>2014</i>	<i>2015</i>
<i>DRAM ½ Pitch (nm) (contacted)</i>	65	57	50	45	40	36	32	28	25

to present day processing techniques and the fact that our devices are shrinking to near atomic dimensions. The ITRS has focused to improve all facets of device manufacturing from advancing materials to lithography. Each facet of device manufacturing from deposition to diffusion is not only dependent on the success of its role, but on the success of each and every step in the process to meet the requirements of device scaling.

## 1.1 Lithography

The process step of focus for this thesis is a part of the lithographic process. Lithography is one of the most frequently used processes in semiconductor device manufacturing. It is instrumental in creating the device features whether it is a capacitor or a transistor on chip. Nearly each step of device fabrication is tied to a lithographic step; so it could be stated that lithography plays the most vital role in device manufacturing.

There are several techniques for lithography, but the premise is the same. A photoresist is deposited over a wafer where it can be exposed to light patterned by a photo mask. Depending on the type of photoresist (positive or negative), the region exposed to the patterned light can be removed or remain depending on the requirements of that step. This removal of photoresist allows for other

processes to be performed on the structure(s) while protecting areas you do not want to process. Resists are designed to react with a specific radiation. Photoresists react with photon radiation of particular frequencies. Calixarenes, the topic of this study, are reactive with electron beam radiation. The thought is that with an electron beam, higher levels of exposure quality at sub-micron dimensions can be achieved simply because the dimensions of the electron beam are typically in the sub-micron regime. The largest drawback of this method, exposure time per area, presently limits the overall usability of this method for large scale production, however this method does have advantages over photolithography which will be discussed next.

Photolithographic techniques use reticles to cast the shadow of information on a resist coated wafer. Each step of device fabrication requires a different reticle, and the photomasks themselves have a finite lifetime. Photomask production is expensive and thus limiting the practicality of this technique. Electron beam apparatus, however, use electromagnetic fields to control the path of electrons, and can be programmed to trace a specific pattern, negating the need for expensive photomask production. This quality allows for a cheaper means of device fabrication and may be more practical for research environments. Lastly, photolithography is approaching its diffraction limited minimum resolution as defined by Rayleigh Equation <sup>3</sup>.

$$R = k_1 \left( \frac{\lambda}{n \sin a_0} \right) \quad (1.1)$$

Where  $R$  is the minimum resolvable size,  $\lambda$  is the radiation wavelength,  $n$  is the refractive index of the material,  $k_1$  and  $a_0$  are parameters dependent on the setup. Modern photolithography utilizes wavelengths of 193 nm along with innovative process environments/materials to reach a minimum resolvable length of 65 nm. In contrast, electron-beam wavelengths can be made considerably shorter thus allowing for a smaller minimum resolvable size due to the directly proportional nature of these two values. The wavelength of an electron can be found using the de Broglie Equation.

$$\lambda_e = \frac{hc}{2m_e c^2 eU} \quad (1.2)$$

Where  $\lambda_e$ , the wavelength of the electron, is dependent upon the accelerating voltage  $eU$  and the constants  $m_e$ ,  $c$ , and  $h$ . Using the National Institute for Standards and Technology's values of the constants<sup>4</sup> ( $hc=1.241$  meV,  $m_e c^2=0.511$  MeV) and a typical SEM accelerating voltage used ( $eU=20$  keV), the wavelength of electrons is  $\lambda_e = 8.68$  pm, or more than twenty thousand times shorter than that of 193 nm photons. Resist molecules are much larger than 8.68 pm as is the spot size of any electron-beam, so the resolution of e-beam lithography is not able to reach this minimum, however, the extremely short wavelength of electrons illustrates one advantage of using them in lithography. The calixarene molecule dimensions are on the order of a nanometer so utilizing electron beam lithography could provide a viable solution in the modern IC era.

Nanometer resolution lithography utilizing electron beam spot sizes at and below 5 nm has been achieved, and as small as single electron devices<sup>5</sup>. Ultimately, for the case of the calixarene, the minimum resolution is restricted to the size of the calixarene monomer  $\sim 1nm$ <sup>6</sup>. This project explores calixarenes developed by the chemistry department here at Texas State. Its focus, using Fourier Transform Infrared spectroscopy is an attempt to determine how well the calixarenes that have been developed respond as a resist material, and to what extent they respond.

## CHAPTER 2

### CHEMISTRY OF CALIX[6]ARENES

Calixarenes are a class of inorganic molecules which are composed of carbon molecules, benzenes, arranged in a closed loop. Benzene belongs to a group called aromatic hydrocarbons, abbreviated as arenes. Calixarenes have a “cup” like resemblance and the Latin name for cup is calix which leads to the name calixarene. The number  $n$  ( $n = 2,3,4,5\dots$ ) of benzenes in the loop denote the different types of calixarenes - calix[ $n$ ]arene. The calixarenes in this study are composed of 6 benzenes which are bonded in a closed loop.

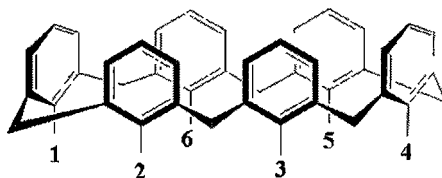


*Figure 2.1: Benzene Ring - Six Benzene rings bonded together to form the Calix[6]arene base.*

Calixarene's six Benzene rings provide a base for further functionalization by the addition of functional groups which can impart specific chemical, physical or structural properties to the molecule. A hexyl functional group is bonded to the Calix[6]arene at opposite ends of the molecule. This facilitates the addition of the xylenyl molecule which acts to lock the calixarene's structure. These can be seen in Figures 2.2 and 2.3.

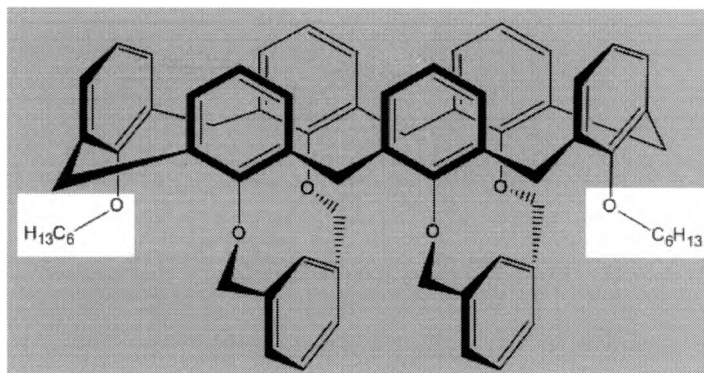


Figure 2.2: Hexyl Groups - Composed of six carbon atoms with 13 hydrogen atoms - facilitates the addition of other functional groups.

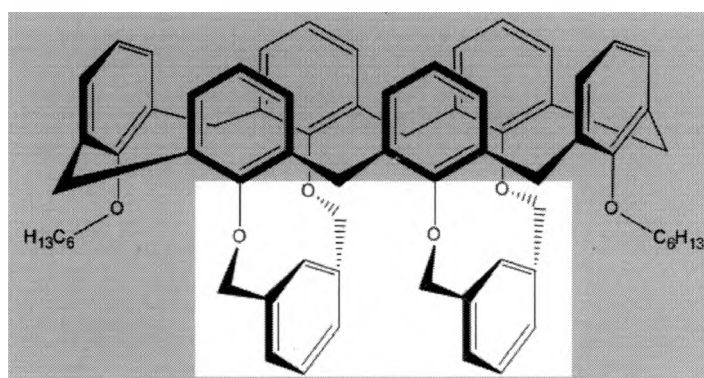
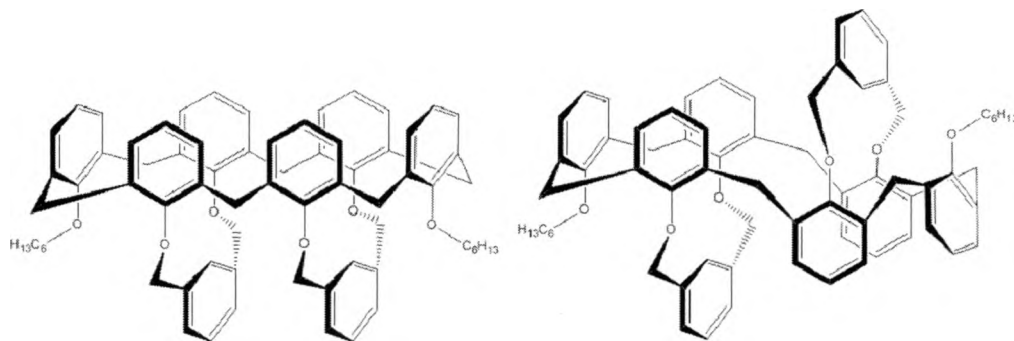


Figure 2.3: Xylenyl Groups - Composed of a benzene group, it is bonded across the molecule, essentially locking the molecule. Addition of the hexyl group shown in Figure 2.2 ensures the xylenyl group can be added in this manner.

Calix[6]arenes can have more than one shape, but still contain the same number,  $n$ , of benzene rings, hexyl and xylenyl groups. These different shapes are referred to as conformations by chemists. The calix[6]arenes in this study take two conformations; known as a cone and 1,2,3-alternate- each shown in Figure 2.4. The two conformations are possible due to the pivoting nature of the molecule. The pivoting is possible due to the methylene ( $CH_2$ ) bridge between each Benzene in the ring. It is not until the hexyl and xylenyl groups are added that the conformation is locked. Both conformations are synthesized during



*Figure 2.4: Cone and 1,2,3 Alternate Conformation. The cone conformation, left, is denoted by the xylene groups being bonded to the same side of the molecule. The 1,2,3- alt conformation contains rotational symmetry with the xylene molecules bonded to opposite sides of the molecule.*

chemical synthesis, however the reaction environment can be tailored to promote one conformation over the other.

Further functionalization by the addition of an allyl group gives the calix[6]arene the ability to bond to other calix[6]arene molecules when exposed to a radiation source. This is otherwise known as polymerization, which is the property under study here. The samples to be studied here vary in their allyl attachment to the calix[6]arene molecule. Allyl groups contain three carbon atoms and five hydrogen atoms arranged in a chain similar to the hexyl chain (Figure 2.5). The number of allyl groups attached to the calix[6]arene may encourage different degrees of polymerization. The calix[6]arenes in this study have either 0,

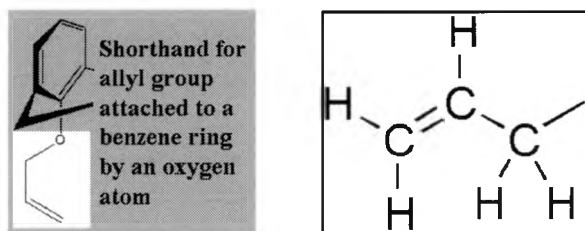


*Figure 2.5: Shorthand and Structural Representation of Allyl Groups.*

2, 4, 6, or 8 allyl groups attached and they are attached to both conformations giving a total of ten variations of calix[6]arenes. To denote each calix[6]arene type throughout the paper note that the number of allyls and the type of conformation are presented as follows. 2C calix[6]arene has 2 allyl groups attached to a cone, C, shaped calix[6]arene. 4A calix[6]arene contains 4 allyl groups attached to the 1,2,3-alternate conformation and so on. All of the conformations are shown in the following: Figure (2.6a-j).

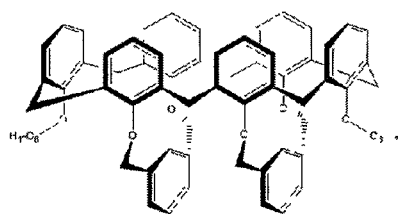


Figure 2.6a: 0C Calix[6]arene

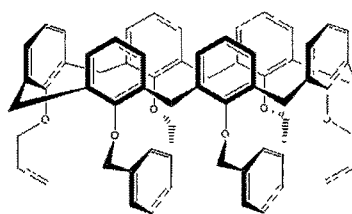


Figure 2.6b: 2C Calix[6]arene

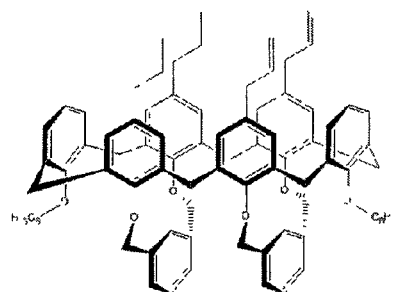


Figure 2.6c: 4C Calix[6]arene

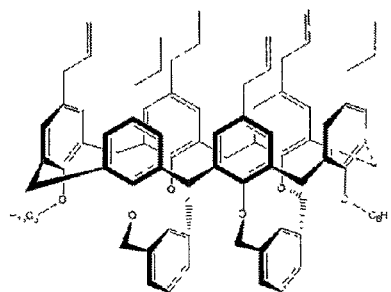


Figure 2.6d: 6C Calix[6]arene

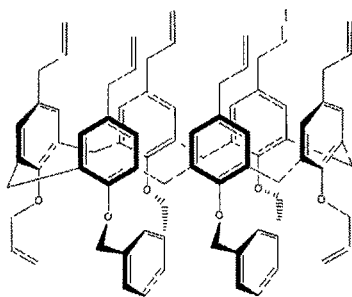


Figure 2.6e: 8C Calix[6]arene

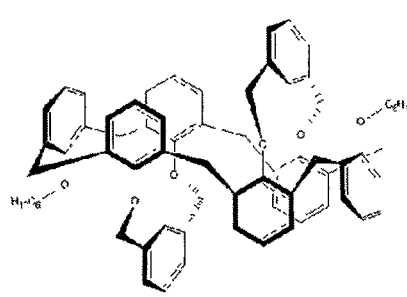
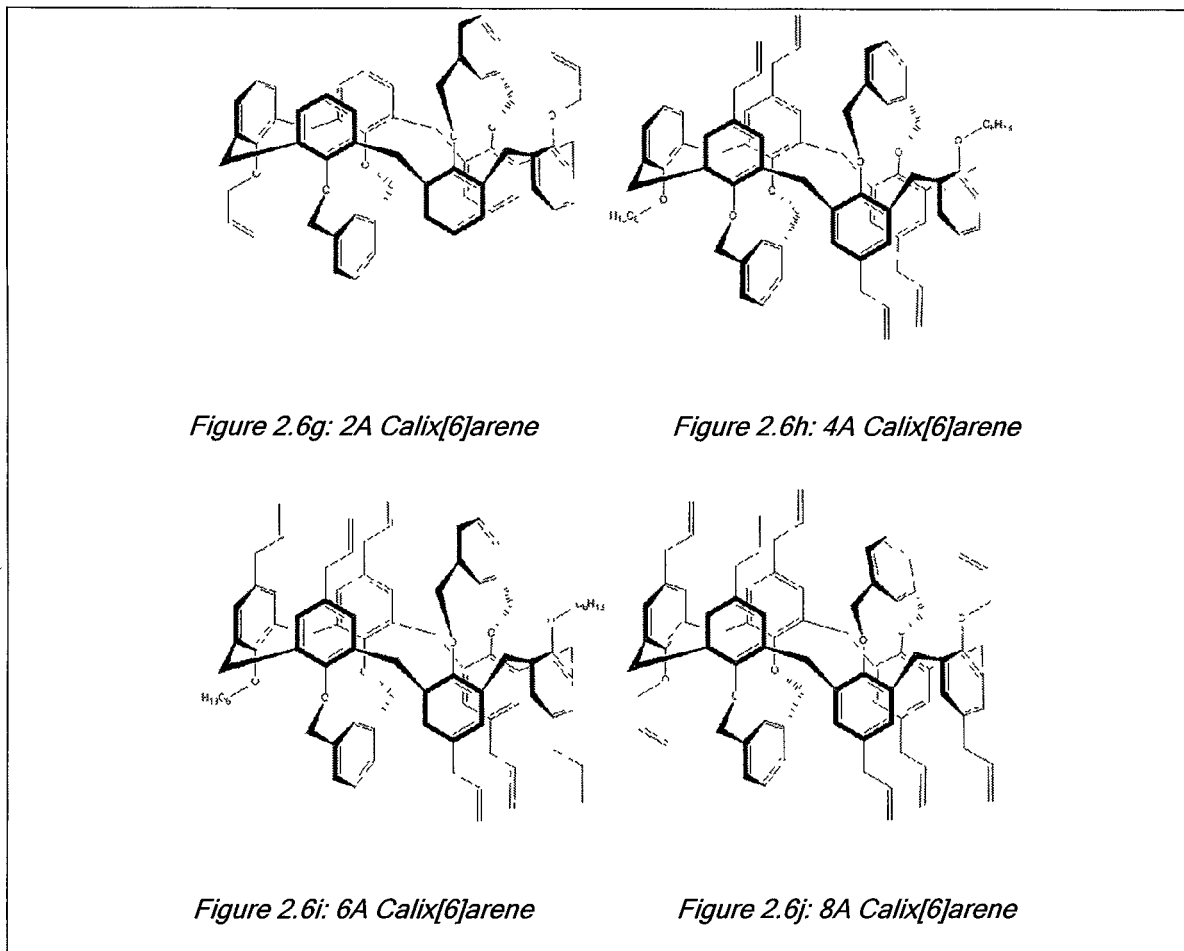


Figure 2.6f: 0A Calix[6]arene



*Figure 2.6(a-j): Ten Calix[6]arene Molecules - Illustrations of the structure of the ten molecules studied in this experiment.*

As seen in Figure 2.5 and 2.6(a-j), there is a double bond between the last two carbon atoms in the allyl group(s) which can bond with other allyl groups if that bond is broken. To break the bond, one needs to impart energy to the molecule, such as an electron beam. Once the bond is broken, it can bond with other allyl groups whether it be intramolecular bonding or more preferably - intermolecular bonding (cross-linking). If more cross-linking occurs it leads to a higher degree of polymerization and thus the calix[6]arene can be more useful as a resist material. These larger structures composed of cross-linked calix[6]arenes

are known as polymers, while the individual calix[6]arene is called a monomer. The polymerization of a calix[6]arene's allyl groups is shown in Figure 2.7.

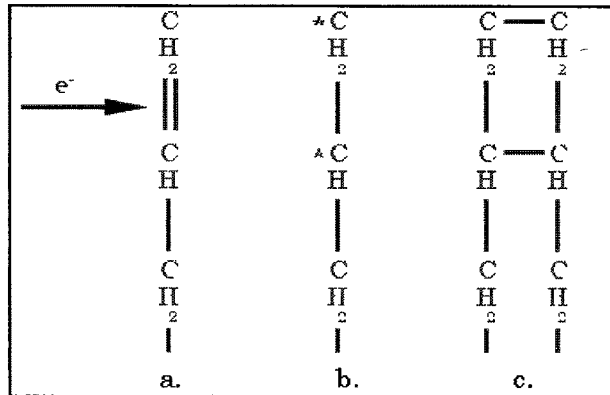


*Figure 2.7: Cross-linking of Allyl Groups - a) an electron is incident upon an allyl molecule which is apart of a calix[6]arene conformation. b) The double carbon bond of the allyl is broken into a single bond and two electrons. c) The newly freed bond may now bond with other free electrons of other allyl groups.*

The nature of inter- and intramolecular linking of allyl is an important aspect of determining how well a calix[6]arene acts as a resist. This quality is directly proportional to the frequency of intermolecular bonding within the material. In other words, the more intermolecular bonds created when exposed to an energy source which increases the amount of calix[6]arene molecules linked together as a polymer, the more likely the calix[6]arene will be useful as a resist material. Detecting the quality of polymerization can be achieved in different ways. One way is to expose the calix[6]arene to electrons and simply try to rinse the calix[6]arene. If it polymerized, the exposed region will bond together forming a region which is highly resistant to being rinsed away. This however tells only one part of the story. This still leaves much to be understood about the

quantity/quality of bonds within the new cross-linked calix[6]arene. The technique of Fourier Transform Infrared Spectroscopy, FTIR, may provide a window in which we can detect the bonding nature within the calix[6]arene (Ch. 3).

## CHAPTER 3

### FOURIER TRANSFORM INFRARED SPECTROSCOPY

Fourier Transform Infrared Spectroscopy, FTIR, has been an important tool to science by providing, among other things, a window into the inner workings of molecule(s). It has served to identify unknown substances, detect band structures of materials, and for the case of this study, will be used to determine if the allyl groups of the calix[6]arene structures do in fact break their double carbon bonds after exposure to radiation, and furthermore attempt to determine the nature of polymerization. More precisely, this study will compare the infrared spectra of each of the ten different calix[6]arene molecules. The spectra will be taken for each molecule pre-exposure and post-exposure and look at the single and double bond regions of the infrared spectra to determine whether or not the bonds of the allyl were in fact broken, and attempt to determine whether or not they bond with other allyl molecules in the calix[6]arene.

#### 3.1 Theory of Infrared Absorption

Atoms and molecules absorb electromagnetic radiation at discrete energy levels. For atoms, the energy absorbed excites the atom causing the electrons to

move to a higher excited state and if enough energy is introduced the electron can be ejected completely. A molecular absorption of radiation initiates a different response within the molecular structure. Absorption of energy for every type of molecule is different and these differences can be attributed to the strength of the bond between atoms within the molecule, the mass of the atoms, and the number of atoms within the molecule. Additionally, higher energies induce other excitations within the electronic band structure of the molecule (Figure 3.1).

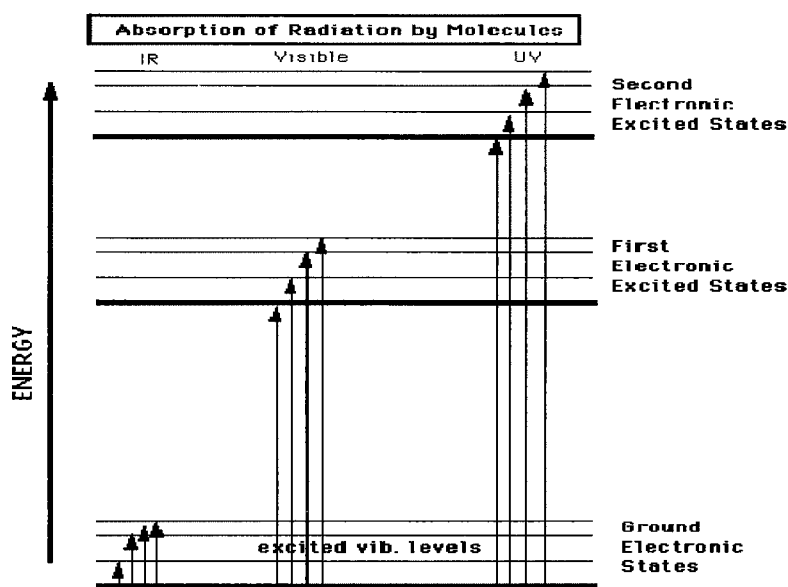


*Figure 3.1: Absorptions of Radiation by Molecules .*

For the case of IR radiation, the energy is not high enough to lift electrons to higher electronic states, however, within each electronic state exists discrete rotational and vibrational energy states. Energy tuned to these rotational and vibrational modes will be absorbed, however if the energy is not in tune with these modes, the energy will not be absorbed by the molecule. Scanning a molecule with a range of energies provides an absorption spectrum depicting which energies a molecule absorbs, the degree of absorption, and what type of

absorption occurs. Figure 3.2 illustrates the reactions of molecules to different types of radiation and expands on the reaction of a molecule to IR radiation. In Figure 3.2, A and B show molecules stretching symmetrically and asymmetrically respectively. C and D show molecular bending in both the plane of the paper and in and out of the paper.

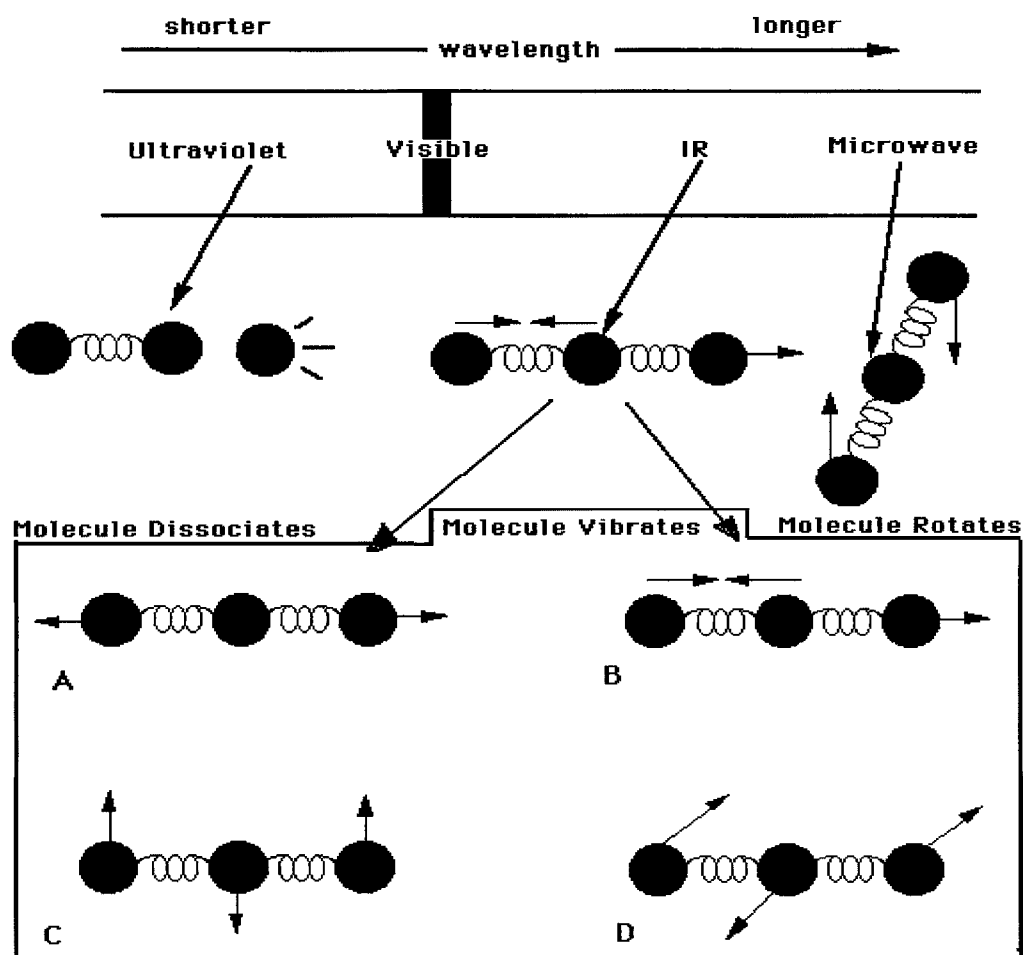


*Figure 3.2: Molecular Energy Reactions and IR Molecular Vibrational Variations<sup>7</sup>.*

The number of atoms in a molecule determines the number of vibrational modes. For any molecule consisting of  $N$  atoms, there are  $3 \cdot N$  degrees of

freedom of which, 3 degrees of freedom are translational (denotes movement of molecule through three dimensional space). There are two basic descriptions of a molecule; linear and nonlinear. A linear molecule contains atoms which are oriented in a line in the same fashion as those in figure 3.2. A nonlinear molecule contains atoms which are not in a line, and contain bond angle less than 180 degrees. For nonlinear molecules, 3 rotational degrees of freedom exist whereas linear molecules have only 2 rotational degrees of freedom. Equations 3.1 and 3.2 describe the number of vibrational modes present in nonlinear and linear molecules respectively. For nonlinear molecules 6 degrees of freedom are subtracted to account for the 3 translational modes plus the 3 rotational modes present. Since linear molecules have only 2 rotational modes and 3 translational modes, 5 degrees of freedom are subtracted.

$$3N - 6 \quad (\text{nonlinear molecules}) \quad (3.1)$$

$$3N - 5 \quad (\text{linear molecules}) \quad (3.2)$$

For example, CO<sub>2</sub>, a linear molecule, has [3(3) - 5 =] 4 vibrational modes of vibration. Large molecules, like the calix[6]arene (C<sub>42</sub>H<sub>36</sub>O<sub>6</sub>), have many vibrational modes. The calix[6]arene molecule has [3(84) - 5 =] 252 vibrational modes. Adding in the vibrational modes of the allyl, hexyl and xylenyl functional groups adds to the confusion. Characterization of so many vibrational modes is a daunting task, however we can partition a molecule into functional groups and neglect the coupling between vibrations of different groups if they are spatially separated or if their force constants differ considerably<sup>8</sup>. If the force constant

between two different bonds differs considerably it means that the energy required to interact with those bonds can differ considerably as well. This allows for differentiating between the absorption bands found on an IR spectrum.

Another point of interest, particularly for this project, relies on the different types of bonds between atoms within a molecule. Three basic bond types are single, double, and triple bonds. To excite the vibrational mode of a triple bond requires more energy than the double bond. Similarly, the double bond requires more energy than the single bond except for the case of any bond with Hydrogen. Hydrogen's exception to this rule can be attributed to its mass. Covalent bonds between two atoms can be compared to a spring. The energy required to compress or stretch a bond between two atoms is expressed in the following equation.

$$\nu = \frac{1}{2\pi c} \left[ \frac{f}{\mu} \right]^{\frac{1}{2}} \quad (3.3)$$

where

$$\mu = \frac{m_1 m_2}{m_1 + m_2} \quad (3.4)$$

Where  $\nu$  is the wavenumber ( $cm^{-1}$ ) which is proportional to the energy,  $c$  is the speed of light,  $f$  is the force constant and  $\mu$  is the reduced mass of the molecule. The force constant ( $f$ ) is similar to that of the spring constant  $k$  found in Hooke's law as it describes the rigidity of the bond. The use of  $\mu$  ensures the center of mass of the molecule is not affected by the vibration. Substituting the expression for the reduced mass (3.4) into equation 3.3 gives <sup>7</sup>

$$\nu = \frac{1}{2\pi c} \left[ f \frac{(m_1 + m_2)}{m_1 m_2} \right]^{\frac{1}{2}} \quad (3.5)$$

It can be seen in equation 3.5 that the larger the masses of the two atoms, the smaller the corresponding frequency. Hydrogen, for example, has the smallest mass of any atom, therefore any bond with hydrogen requires more energy to induce molecular vibrations. Equation 3.5, however, only holds for single bonds. Double bonds and triple bonds between molecules can be compared to springs in parallel. The force constant for two springs in parallel (double bond) is the only factor that changes from a single bond to a double bond. The equivalent force constant,  $f_{eq}$ , for a double bond can be expressed as

$$f_{eq} = f_1 + f_2 \quad (3.6)$$

and for the triple bond

$$f_{eq} = f_1 + f_2 + f_3 \quad (3.7)$$

Where  $f_n$  ( $n = 1,2,3$ ) represents the force constant of a particular bond number. Replacing 3.6 and 3.7 into equation 3.5 accounts for multiple bonds between atoms.

$$v = \frac{1}{2\pi c} \left[ (f_1 + f_2) \frac{(m_1 + m_2)}{m_1 m_2} \right]^{\frac{1}{2}} \quad (3.8)$$

and

$$v = \frac{1}{2\pi c} \left[ (f_1 + f_2 + f_3) \frac{(m_1 + m_2)}{m_1 m_2} \right]^{\frac{1}{2}} \quad (3.9)$$

Listed in Table 3.1 are the typical IR regions where each bond is excited into its various vibrational modes. The carbon=carbon double bond of the allyl group

*Table 3.1: IR absorption regions of basic bond structures*

3700 - 2500 cm <sup>-1</sup>	Single bonds to Hydrogen
2300 - 2000 cm <sup>-1</sup>	Triple bonds
1900 - 1500 cm <sup>-1</sup>	Double bonds
1400 - 650 cm <sup>-1</sup>	Single bonds (other than Hydrogen)

attached to the calix[6]arene can be broken by an electron beam or as mentioned earlier in this section, ultra-violet radiation. Once the bond is broken it is free to bond with with other allyls, however, these new bonds are now carbon-carbon single bonds, as discussed in Chapter 2 (Figure 2.7). Figure 3.3, below, shows regions where infrared absorption of both the carbon=carbon double bond and carbon-carbon single bonds will occur. Since the calix[6]arene becomes polymerized when C=C double bond of its allyl group(s) is broken and then attached to other similarly broken allyl groups forming a C-C single bond, we can look at the IR spectrum pre-exposure and compare it to the spectrum of a post exposed sample and determine whether or not a polymerization has occurred.

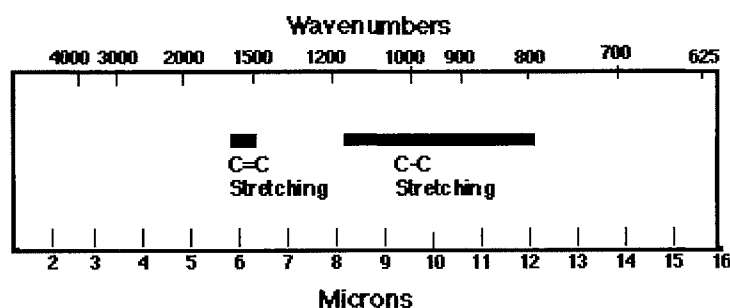


*Figure 3.3: C=C and C-C stretching regions of an IR spectra<sup>7</sup>.*

### 3.2 Theory of FTIR

Fourier Transform Infrared Spectroscopy (FTIR) is a technique used to measure the absorption of energy by a substance. The physical properties of the components of a FTIR spectrometer are key to understanding the results given by the spectrometer. The most important component of the FTIR spectrometer is the Michelson Interferometer. A Michelson interferometer is composed of a light source, beamsplitter a fixed mirror, a moveable mirror, a detector and a sample compartment as shown in Figure 3.4.

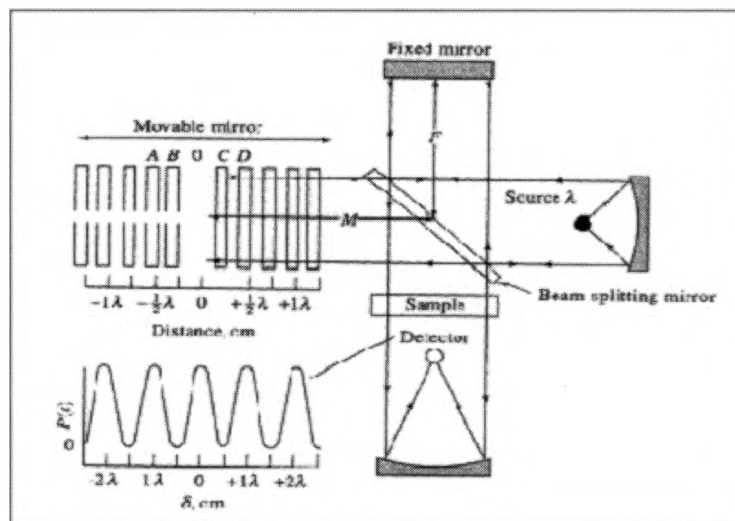


Figure 3.4: Michelson Interferometer<sup>8</sup>.

The interferometer uses a light source, which contains all the infrared frequencies. Light from a source is split into two beams by a beamsplitter. One of the split beams is incident on a fixed mirror and the other beam is incident on a moving mirror where both beams are reflected off their respective mirrors back to the beam splitter and recombine either destructively or constructively. Half of the beam is sent back to the source while the other half is directed through the sample of interest and then to the detector. The detector records the signal in the

form of an interferogram, which contains encoded information about the sample. After the interferogram is completed, the computer can compute the Fourier Transform of the interferogram, which gives a plot of intensity versus frequency for the spectrum in the form of reflectance, absorbance or transmittance intensities versus wavenumber ( $\text{cm}^{-1}$ ). The use of wavenumbers,  $\tilde{\nu}$ , in spectroscopy is due to its convenience. It is directly proportional to the energy of the photon,  $E_p$ , and frequency,  $f$ , and inversely proportional to wavelength  $\lambda$ . The energy of a photon is expressed as follows <sup>9</sup>:

$$E_p = \frac{hc}{\lambda} = hf = hc\tilde{\nu} \quad (3.10)$$

$$h = \text{Plank's constant} = 6.636 \times 10^{-34} \text{J} \cdot \text{s} = 4.136 \times 10^{-15} \text{eV} \cdot \text{s}$$

The process by which the Michelson interferometer creates the frequencies of light is best understood by first considering an ideal situation where a source produces an infinitely narrow beam with rays all parallel to each other (collimated). The ideal beamsplitter is non-absorbing, reflecting and transmitting exactly 50% of the incident source. The beam is then incident either on the movable mirror or the fixed mirror. As the mirror moves, it creates a phase difference compared to the beam incident on the fixed mirror. When the beams return to the beamsplitter, they either interfere constructively or destructively depending on the retardation ( $\delta$ ) of the mirror, also known as the optical path difference. When the mirrors are equidistant from the beamsplitter, there is zero retardation and the beams interfere constructively and the detector receives the

sum of the intensities while no light is returned to the source. When the mirror is displaced by a distance of  $1/4\lambda$ , the optical path difference is  $1/2\lambda$  and the beams are completely out of phase, interfering destructively. If the mirror is moved with a constant velocity, The signal at the detector will vary sinusoidally with the minimum occurring at each multiple of  $1/2\lambda$ . This property known as temporal coherence is the heart of the FTIR operation and allows for extraction of energy spectra. Knowing how the interference pattern changes over time and times relationship with frequency, frequency being the inverse of time, we can use a Fourier Transform to convert from a time domain to a frequency domain. To describe how the process works, it is simplest to first consider a monochromatic source which produces a perfectly collimated, infinitely narrow beam. The intensity of the beam at the detector  $I'(\delta)$  at mirror retardation  $\delta$  is given by the following<sup>10</sup>.

$$I'(\delta) = 0.5I(f) \left\{ 1 + \cos 2\pi \frac{\delta}{\lambda} \right\} \quad (3.11)$$

$$= 0.5I(f) \{ 1 + \cos 2\pi \tilde{\nu} \delta \} \quad (3.12)$$

$$\tilde{\nu} = \frac{1}{\lambda} \quad (\text{wavenumber, } cm^{-1})$$

where  $I(f)$  is the intensity of the source as a function of frequency and 0.5 is the ideal beamsplitter correction factor.  $I'(\delta)$  contains both a dc component,  $0.5I(f)$ , and an ac component,  $0.5I(f) \cos 2\pi \tilde{\nu} \delta$ . For spectroscopic measurements, only the ac component is important. This component is referred to as the

interferogram. The interferogram from a monochromatic source is given by the equation

$$I(\delta) = 0.5I(\tilde{\nu}) \cos 2\pi\tilde{\nu}\delta \quad (3.13)$$

This however is not the entire picture. First, it is impossible to create a beamsplitter which can divide a beam into 50% reflected and 50% transmitted. A new factor must be introduced to account for the non-ideality. This new factor  $H(\nu)$  represents the beamsplitter efficiency and is lower than unity. Included in this value are the detector response and the characteristics of the amplifier. Many infrared detectors and amplifiers respond differently to different frequencies. These are both frequency dependent and affect the intensity of the signal. The wavenumber-dependent correction factor is a multiplier of the intensity and affects the interferogram as follows.

$$I(\delta) = 0.5H(\tilde{\nu})I(\tilde{\nu}) \cos 2\pi\tilde{\nu}\delta \quad (3.14)$$

The value  $0.5H(\tilde{\nu})I(\tilde{\nu})$  can be set equal to  $\beta(\tilde{\nu})$ , a single beam spectral intensity expression containing all the information of the various components of the spectrometer.

$$I(\delta) = \beta(\tilde{\nu}) \cos 2\pi\tilde{\nu}\delta \quad (3.15)$$

It was mentioned previously that the IR spectrum is obtained by converting from a time domain to a frequency domain. Expression 3.15 does not directly contain any information for either time or frequency, however a couple of modifications can be made to account for both. To do so first we must know how the intensity varies as a function of time -  $I(t)$ . As the mirror moves, the intensity of the signal at the detector varies depending on the retardation of the mirror. The retardation at some time after zero retardation is

$$\delta = 2vt \quad (3.16)$$

$v$  – mirror velocity

Replacing  $\delta$  into 3.15 yields

$$I(t) = \beta(\tilde{\nu})\{\cos 4\pi\tilde{\nu} \cdot vt\} \quad (3.17)$$

At zero retardation, when  $t = 0$ , we find that the intensity of the interferogram is a maximum

$$I(t) = \beta(\tilde{\nu})\{\cos 4\pi\tilde{\nu} \cdot v \cdot 0\} \quad (3.18)$$

$$I(t) = \beta(\tilde{\nu}) \quad (3.19)$$

which is simply the intensity of the source coupled with the beamsplitter efficiency, detector response, and amplifier response. When  $t = \frac{\delta}{2v}$ , where  $\delta =$

$\frac{1}{2}\lambda$ ,  $I(t)$  is now at a minimum. Note\*  $\tilde{\nu} = \frac{1}{\lambda}$

$$I(t) = \beta(\tilde{\nu}) \left\{ \cos 4\pi\tilde{\nu} \cdot v \frac{\lambda}{4v} \right\} \quad (3.20)$$

$$I(t) = -\beta(\tilde{\nu}) \quad (3.21)$$

3.21 and 3.19 are both cases where the waves interfere constructively. If the mirror is displaced a distance of  $\delta = \frac{\lambda}{4}$ , at  $t = \frac{\delta}{2v}$ , we have a case where the waves interfere destructively canceling each other out.

$$I(t) = \beta(\tilde{\nu}) \left\{ \cos 4\pi\tilde{\nu} \cdot v \frac{\lambda}{8v} \right\} \quad (3.22)$$

$$I(t) = 0 \quad (3.23)$$

The sinusoidal characteristics of the monochromatic interferogram are easy to see in this manner, however, spectrometers use more than one frequency of light. These polychromatic sources result in an interferogram containing information about every frequency of light produced by the source. When the source is a continuum, the interferogram is given by the integral

$$I(\delta) = \int_{-\infty}^{\infty} \beta(\tilde{\nu}) \cos 2\pi\tilde{\nu}\delta \cdot d\tilde{\nu} \quad (3.24)$$

which contains information about  $I(\delta)$  for every possible wavenumber. To solve for  $\beta(\tilde{\nu})$ , which contains information with regards to  $I(\tilde{\nu})$ , we can use the cosine Fourier transform and get the other half of the pair.

$$\beta(\tilde{\nu}) = \int_{-\infty}^{\infty} I(\delta) \cos 2\pi\tilde{\nu}\delta \cdot d\delta \quad (3.25)$$

Noting that  $I(\delta)$  and  $\cos 2\pi\tilde{\nu}\delta$  are even functions, 3.25 becomes

$$\beta(\tilde{\nu}) = 2 \cdot \int_0^{\infty} I(\delta) \cos 2\pi\tilde{\nu}\delta \cdot d\delta \quad (3.26)$$

3.24, 3.25 and 2.26 together show that one could measure the entire spectrum, but to do so one would be required to have an interferometer that had the ability to scan an infinite distance and a digital computer that could create an interferogram using infinitesimal intervals of retardation. Further understanding of this requires elements of finite resolution techniques which take into account the problem of infinite moving mirrors and infinitesimally small sampling of mirror retardation by multiplying the interferogram by a boxcar truncation function. This yields a spectrum upon Fourier transformation that is the convolution of the FT of  $I(\delta)$ , with the FT of  $D(\delta)$ ,  $D(\delta)$  representing the boxcar truncation function.

$$\beta(\tilde{\nu}) = 2 \cdot \int_0^{\infty} I(\delta)D(\delta) \cos 2\pi\tilde{\nu}\delta \cdot d\delta \quad (3.27)$$

In summary the Michelson interferometer creates a time dependent wave, which can be converted to a frequency domain by means of a Fourier transform. The transformation of mirror retardation to frequency domain  $I(\delta) \xleftrightarrow{FT} \beta(\tilde{\nu})$  allows us to observe absorptions of a sample over an energy range in FTIR

spectrometers. When the spectrum of the source is monochromatic, performing the Fourier transform is simple since the amplitude and wavelength can be measured by direct means. For the case of polychromatic sources, the interferogram is the result due to the combination of all the interferograms for each wavenumber of the source. Polychromatic sources require a digital computer to perform the transforms for all of the frequencies.

A typical scan time, scan time referring to the time it takes to record the interferogram of the frequency range requested, is one second. The FTIR spectrometers can be programmed to take many scans in succession, record a spectra per scan and average the data over as many scans as is necessary to create an accurate spectral picture of the sample in question in considerably less time than dispersive techniques. Other advantages of using FTIR spectrometers include<sup>7</sup>.

- It is a non-destructive technique.
- It provides a precise measurement method, which contains no external calibration.
- Mechanically simple.

- Jacquinot's Advantage: resolution is not limited by the aperture widths necessary for dispersive spectrometers. Can increase light throughput by 10 - 200 fold.
- Multiplex Advantage ( Fellgett's Advantage): Signal from source is continuously monitored which increases the signal to noise (S/N) ratio. The FTIR spectrometer can make many successive scans over a short period of time and take the time average to increase the S/N ratio.

FTIR spectroscopy is a useful tool for analyzing energy absorptions in materials. It is by far the easiest way to determine the band gap and transitional energies of a material and this makes FTIR especially critical to the semiconductor industry.

## CHAPTER 4

### EXPERIMENT AND RESULTS

#### 4.1 Calix[6]arene Preparation

The Calix[6]arenes used in this study were created by the Chemistry Department here at Texas State by Dr. Blanda and his research group. The resist formula consists of 1% calix[6]arene powder in a chlorobenzene solvent. Chlorobenzene properties such as its low melting point, toxicity and reactivity are well understood so it is well suited to be used as the primary solvent in this study. The resists were mixed using approximately 5 - 15 mL chlorobenzene to a vessel on a tared scale so as to only include the weight of the calixarene and not the vessel. The scale was then tared again and the calixarene powder was added until it weighed 1% (generally about  $\frac{1}{5}$  of a gram) of the measured chlorobenzene. Using this method alleviates the need to consider variable calix[6]arene density or calculating molecular weight for each compound<sup>3</sup>.

#### 4.2 Calix[6]arene Deposition

The calixarenes were deposited on 100 mm silicon wafers using a programmable wafer spinner (Figure 4.1). Using the 100mm silicon wafers serves two functions for this study. One is it provides many samples for study as the

wafer can be broken into smaller pieces and the other is silicon's high transparency to the IR region of the electromagnetic spectrum. The wafer is placed on the vacuum chuck of the spinner and the vacuum switch located on the spinner control unit is turned on. Next the form which forces the wafer to be centered on the chuck is removed and the lid is closed. Three mL



*Figure 4.1: Wafer Spinner.*

of resist are pulled into a syringe, the syringe is turned upwards and a 0.5mm filter is placed between the needle and vessel. The spinner is then turned on and the contents of the syringe are deposited onto the wafer. The wafers were spun at 3000 rpm for 30 seconds. This step is sandwiched between a 15 second ramp up stage and a 15 second ramp down stage which limits stress on the wafer. Once the program is finished, the wafer was removed and set on a hot plate at 100°C for 60 seconds. Baking the sample evaporates the chloroform in the resist leaving only a thin film of calix[6]arene on the substrate. The sample is then allowed to dry before being cleaved into smaller samples. This step was repeated for each of the nine calix[6]arene conformations. Note\* At this stage one can take ellipsometry measurements to determine the film thickness, however for this study, the step was skipped. In a previous elipsometry study conducted by Russell Kendall, deviations of film thickness using the same spinner and slightly

different spinner program parameters yielded a 20% variation across the surface of the wafer. While this variation should not affect polymerization it does affect the FTIR results discussed later in this chapter.

### 4.3 UV Exposure of Calix[6]arenes

Although these resists are designed for electron-beam exposure, a UV light source was experimented with to determine if the resists would react to such an energy source. This seems counter-intuitive, however, the FTIR technique used requires a large area exposure which would be difficult to obtain using the scanning electron microscope. The samples were exposed using a Spectra Physics 75 Watt Xenon lamp which emits UV light spanning the entire UV up to 190 nm. Each sample was exposed for 2, 5, 10, 20 and 1000 minutes at 30 Watts. The Intensity was measured using a Metrologic photometer. Between each successive exposure a new FTIR spectra was recorded.

### 4.4 FTIR Analysis

The spectra were recorded using a Nicolet 6700 series FTIR spectrometer. This technique, while very informative, requires many small steps to ensure the IR spectra recorded are in fact the true spectra of the sample being studied. A more detailed operation guide that explains in more detail some of the idiosyncracies that pertain to FTIR and a simple guide to the OMNIC computer interface can be found in the Appendix.

The spectra were collected using the same parameters to provide some continuity throughout the experiments. Many factors are beyond full user control,

such as  $CO_2$  and  $H_2O$  levels and fluctuations in the atmosphere surrounding the optics and path of the beam, however steps were taken to limit the affects of such gases. Before any measurements were attempted, the spectrometer was purged using  $N_2$  gas. The spectrometer was purged for at least 2 hours before any spectra were recorded.  $N_2$  is a homonuclear molecule which does not absorb infrared radiation. Saturating the local atmosphere with Nitrogen limits the amount of other gases present, which can cause unwanted absorptions. Other candidates for purging could be the noble gases since they do not bond with other atoms to form a molecule<sup>11</sup>. No bond means no vibration.

Nitrogen serves two roles in the experiment. The gas form, as mentioned previously, purges the system, and the liquid form is a cooling medium for the MCT (Mercury Cadmium Telluride) detector. The MCT detector operates poorly at room temperature due to thermal excitations so it must be cooled to minimize these affects. Liquid Nitrogen has a temperature of about 77 degrees Kelvin and is well suited for this detector. Other mediums can be used, such as liquid Helium (~ 3 degrees K), to further reduce the thermal affects, but for this study it was unnecessary. Once the system was purged, the detector was filled with liquid Nitrogen and allowed to reach an equilibrium temperature. While no thermocouples were employed to measure the temperature of the detector, the interferogram display in the experiment setup tab was used to determine the state of the detector. Once the interferogram reached a maximum intensity, the detector was at temperature ready for use (Figure 4.2). The Nicolet 6700 comes equipped with 3 choices for beamsplitter. Figure A.4 highlights the beamsplitter/detector combinations possible and provides combination

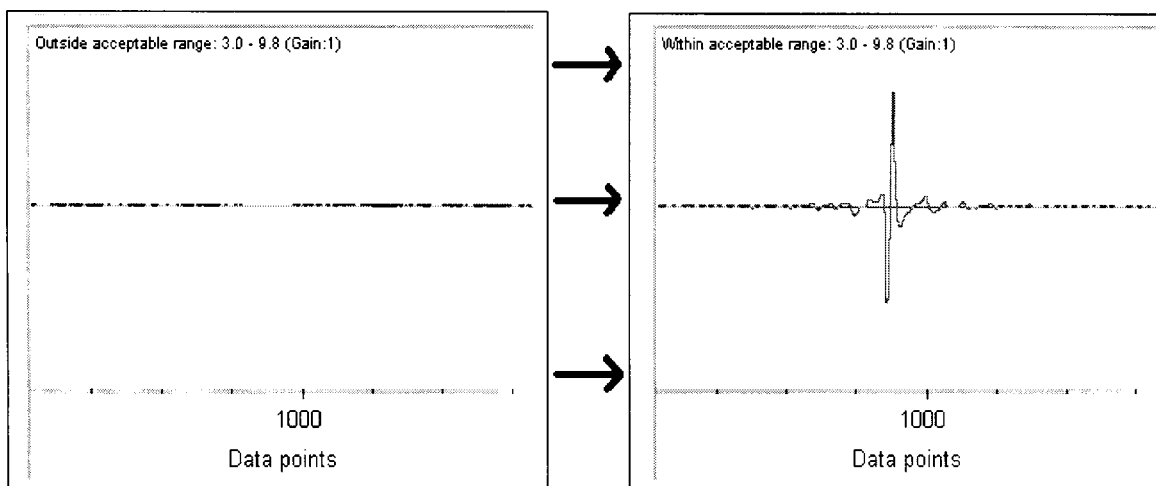


*Figure 4.2: Interferogram and the MCT detector. The picture on the left shows the interferogram generated using a room temperature MCT. The one on the right shows the interferogram once the MCT has been cooled by liquid nitrogen.*

Performance with respect to spectral range. The KBr beamsplitter was chosen because the MCT/KBr combination is best suited for the Mid IR range. This combination provides a detector signal large enough to allow the beamsplitter to be aligned. Once the combination was chosen, the OMNIC interface automatically adjusted the spectral range to the optimum settings (650 - 4000  $\text{cm}^{-1}$ ). The Gain was set to Autogain, but generally remained at the lowest setting - 1. Larger Gain settings amplify the detector signal, but since the MCT is sensitive, raising the gain only degrades spectral quality. Another method employed to improve spectral quality was to shrink the aperture size to a setting of 7. This limited the amount of light incident on the detector thus preventing signal saturation. The mirror velocity was set to 1.8988  $\frac{\text{cm}}{\text{s}}$ . For each spectra recorded, 32 scans at 4  $\text{cm}^{-1}$  resolution were taken and averaged.

Before each sample spectra was recorded a background spectrum was recorded. Collecting a background is necessary to record the spectra of the

spectrometer's atmosphere and contributions from the various components the IR beam may come in contact with. Included in the background spectra was bare Silicon. Silicon was attached to a cardboard slide with a hole in it using two-sided tape and placed in the path of the beam. Collecting a background with Silicon included ensures that only the spectra of the Calix[6]arene appeared in the sample spectra. While Silicon is mostly transparent to the IR it does absorb some IR energies. Figure 4.3 shows the difference between a background collected with and without Si. Notice the difference between them resides in the fingerprint region of the spectrum,  $600\text{-}1200\text{ cm}^{-1}$ . If unaccounted for the spectra could be predominately Si due to the thickness of the silicon compared to the thickness of the calix[6]arene film.

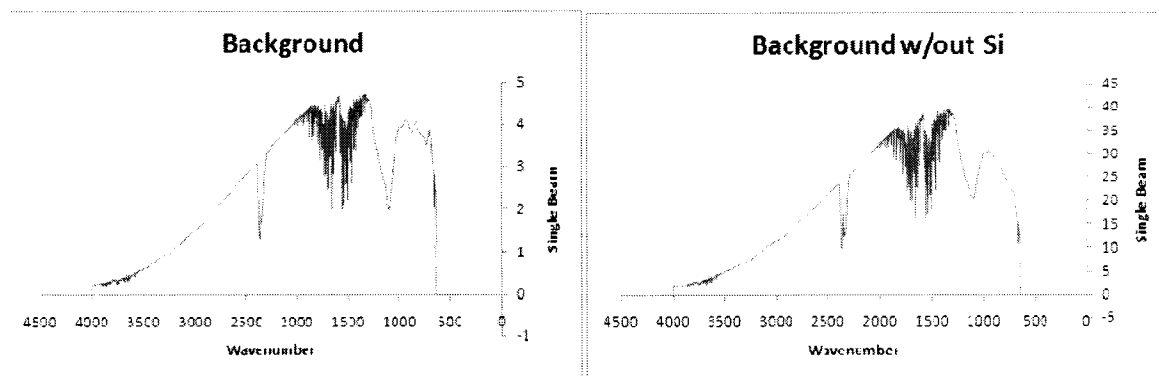


*Figure 4.3: Background Spectrum with and without Silicon.*

This background contains absorptions from the various components of the spectrometer and the atmosphere. The doublet at approximately  $2400\text{ cm}^{-1}$  is a result of  $\text{CO}_2$ . The spiked regions from  $800\text{ - }2000\text{ cm}^{-1}$  and  $3500\text{ - }4000\text{ cm}^{-1}$  are absorptions due to water and the bell shape absorption which spans most of the spectra reflects the detector response and the output of the source. To determine whether or not the system is purged properly, a sample scan can be

taken after the background scan. If the system is purged properly the resulting spectra should be at 100% Transmittance or zero Absorbance. While it is very difficult to achieve a perfect 100% transmittance or zero absorbance at atmospheric pressure, values from 98-102% transmittance or 0 - 0.5 are acceptable values. This is due to fluctuations in the atmosphere from the time the background is taken to the time the sample scan is taken. Figure 4.4 shows a result of such a procedure.

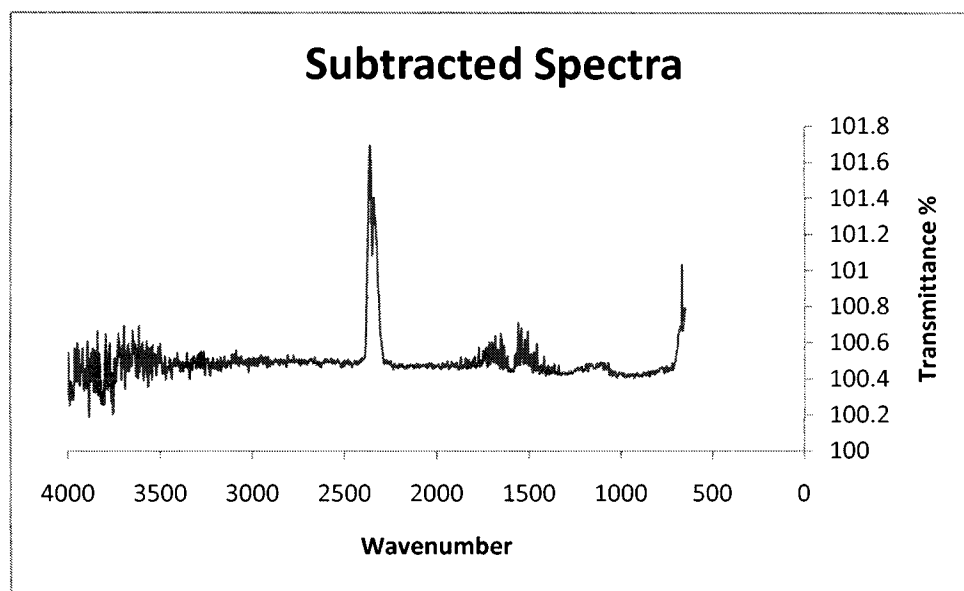


*Figure 4.4: Subtracted Spectra Test.*

A flat line 100% transmittance spectra would be ideal, however, as mentioned before, obtaining such a spectra is difficult. Water and carbon dioxide levels change from one moment to the next and are present in spectra even if they were accounted for in the background. Generally the effect is minimal, however when measuring very thin samples where the absorptions are small, they can degrade the quality of the spectra considerably. While these effects had

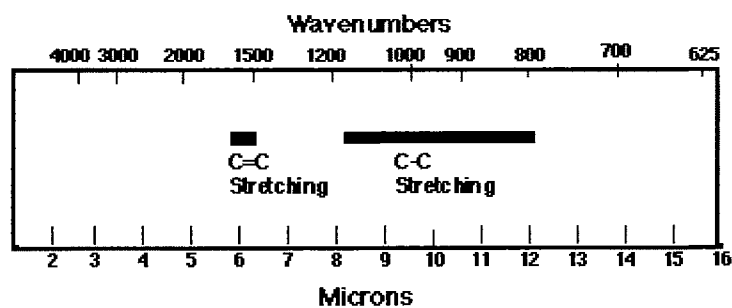
minimal effects on this experiment, on a couple occasions this effect was insurmountable.

Another problem commonly encountered is negative absorbance or transmittance percentages > 100%. This can be attributed to deviations of substrate thickness. Silicon can bond with oxygen, forming a thin film of  $SiO_2$  between the Silicon and calix[6]arene. The thicknesses of the oxide layer on the plain Si sometimes varies with the oxide level on the calix[6]arene sample substrate. If this is the case then there will naturally be a slight deviation across the spectrum which can result in negative spectra as well as spectra shifted slightly upwards in areas where Silicon dioxide absorbs IR light. For this study, this effect was encountered occasionally, however, it was overcome by moving the sample so that the beam intersected a different region and taking a new spectrum. A point to be noted is that the region of the IR spectra where this most commonly occurred, was not in the region where the calix[6]arene experienced IR absorptions.

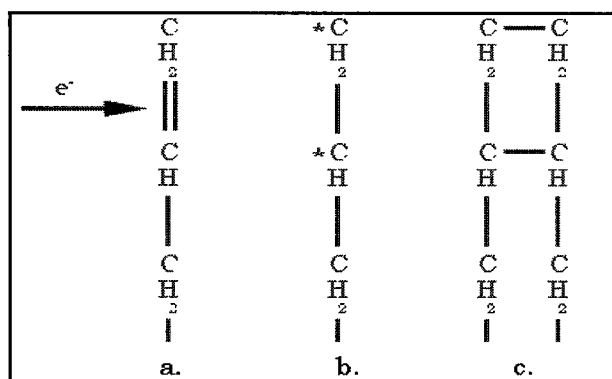
#### 4.5 IR Spectra

The calix[6]arenes studied here were the species 2A, 8A, 2C, and 8C. These were chosen for two reasons. In a previous study using the SEM's electron beam to expose the samples conducted by Russel Kendall, These species resisted xylene development better than the 4 (A and C) and the 6A species. The 6C species is still under development and the 0 (A and C) in theory will not polymerize as they possess no allyl groups to fulfill the functionality requirements of polymerization. The choice of the 2 and 8 (A and C) species, if polymerization

were to be detected, would give us a picture of the two extremes. One being the least amount of polymerization (2A and 2C), and a high degree of polymerization (8A and 8C). Initially I believed the 2A species would be the most likely to show evidence of polymerization due to the structure of the molecule. There is no possible way for the allyl to bond intramolecularly with another allyl; so if the bond were to break, it would have to bond with an adjacent calix[6]arene's allyl, however the 8 species have a higher probability of polymerization do to the number of allyls present. Here we will see the resulting spectra of each species at each time step of exposure. The regions of interest are recapped in Figure 4.5. The original idea was to see if there existed changes in the IR spectra due to polymerization of calix[6]arenes. These changes could occur when the double carbon bond of the attached allyl groups break and bond intermolecularly with other broken double carbon bonds of adjacent calix[6]arene molecules forming a single carbon bond between the two calixa[6]arene molecules. This is revisited in Figure 4.6.

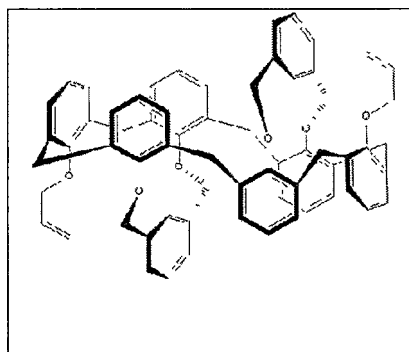


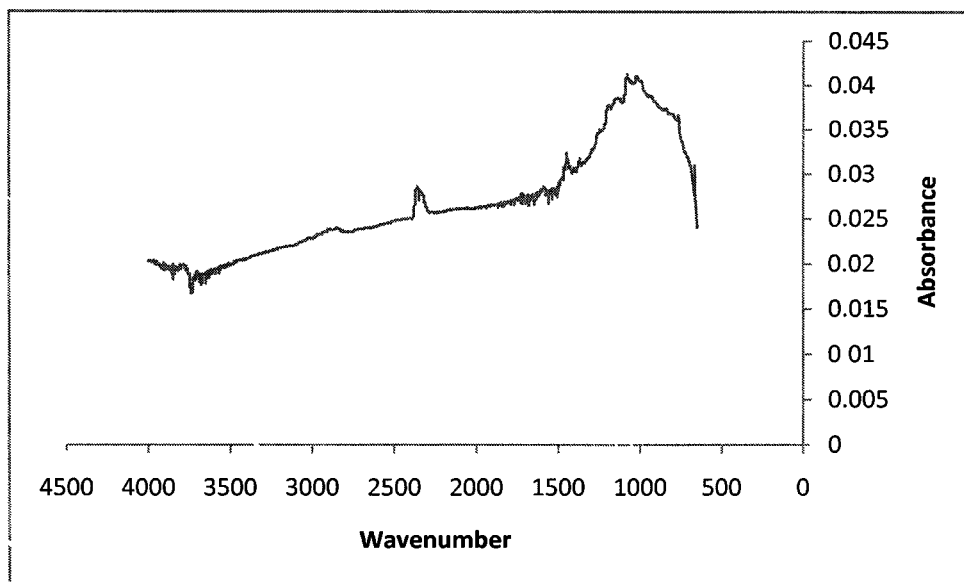
*Figure 4.5: C=C and C-C stretching regions of an IR spectra<sup>7</sup>.*



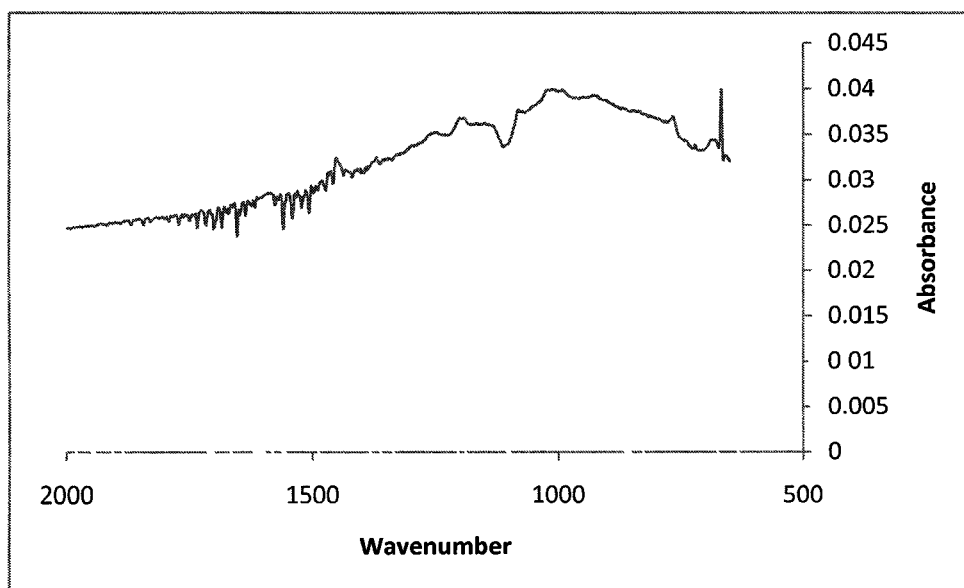
*Figure 4.6: Cross-linking of Allyl Groups - a) an electron is incident upon an allyl molecule which is a part of a calix[6]arene conformation. B) The double carbon bond of the allyl is broken into a single bond and two electrons. C) The newly freed bond may now bond with other free electrons of other allyl groups<sup>3</sup>.*

## 2A

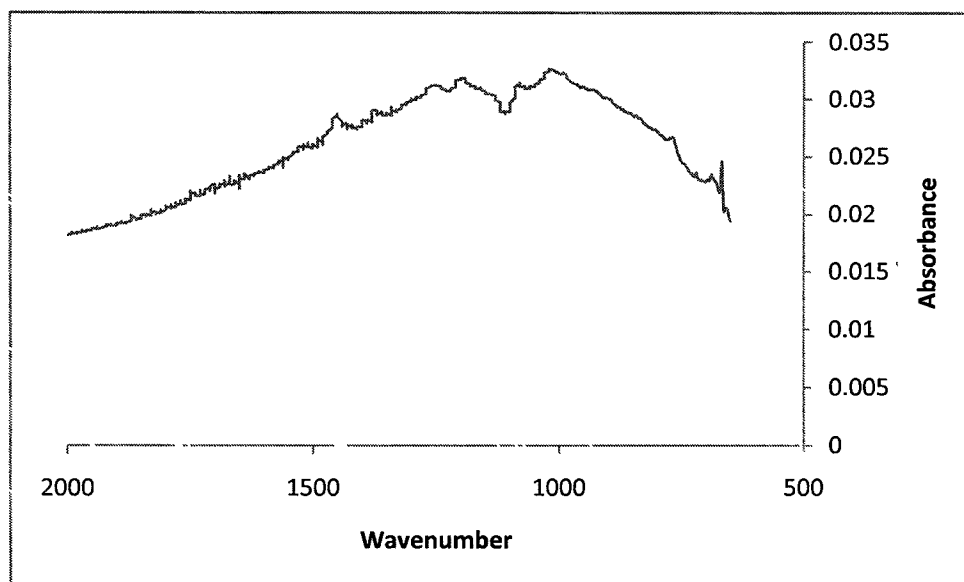




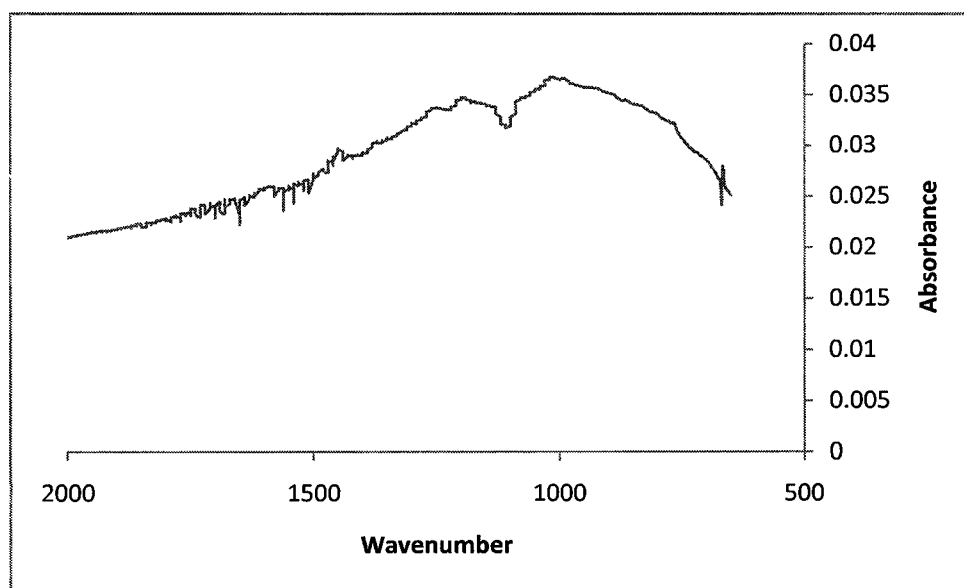
*Spectrum 4.1: Unexposed*



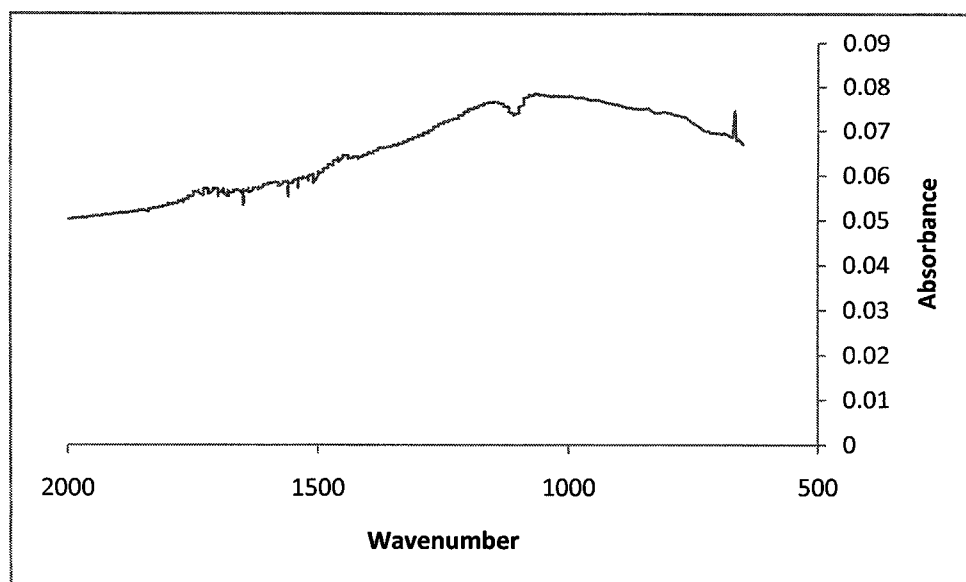
*Spectrum 4.2: 2 minute exposure*



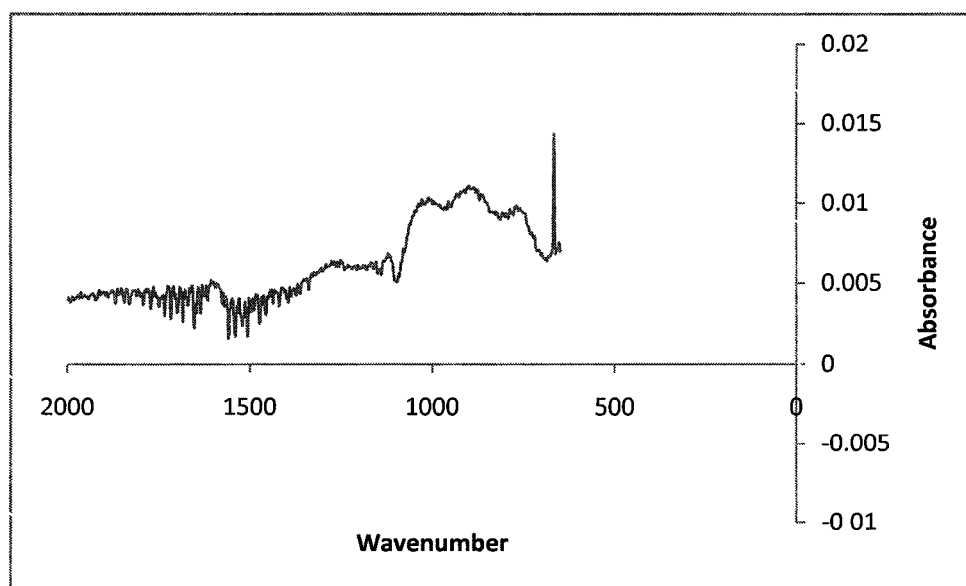
*Spectrum 4.3: 5 minute exposure*



*Spectrum 4.4: 10 minute exposure*



*Spectrum 4.5: 20 min exposure*



*Spectrum 4.6: 1000 minute exposure*

The 2A species experienced the most dramatic change between the 20 min exposure and the 1000 minute exposure. Spectra 4.1 through 4.5 did not experience any dramatic absorption changes and the spectra did not have any absorptions showing evidence of C=C bonds or C-C bonds. The lack of

absorptions indicated that the 2A species may be transparent to IR absorptions or that the region of the sample tested did not contain calix[6]arene molecules. One clue that there may not have been a calix[6]arene present is to look to the absorption spectrum of the base molecule of the calix[6]arene - Benzene (Figure 4.6)

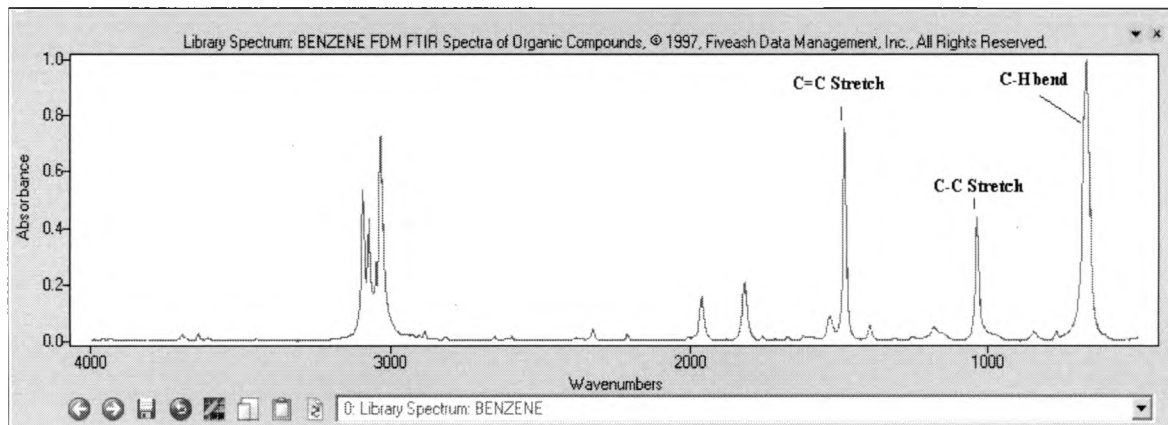
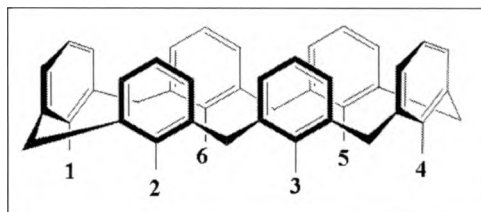


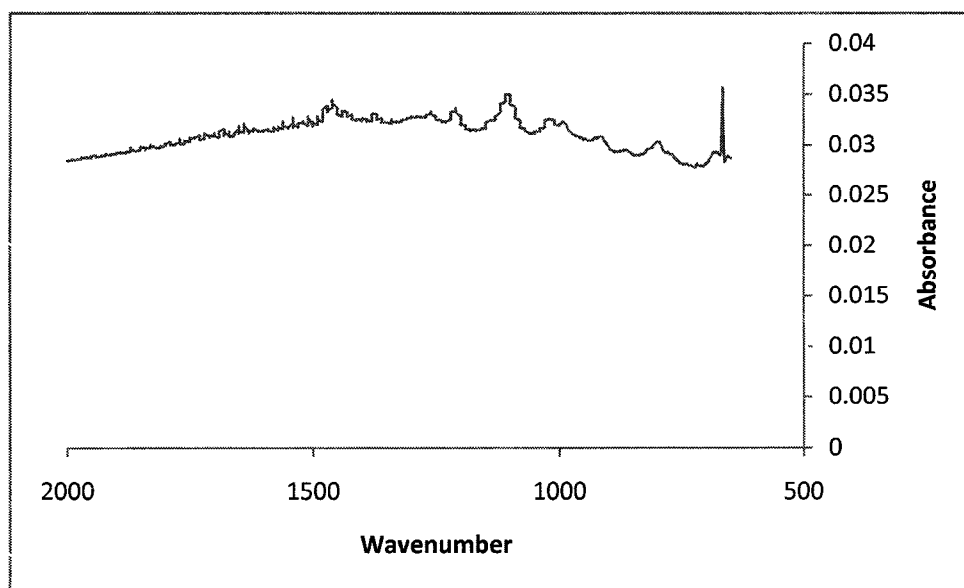
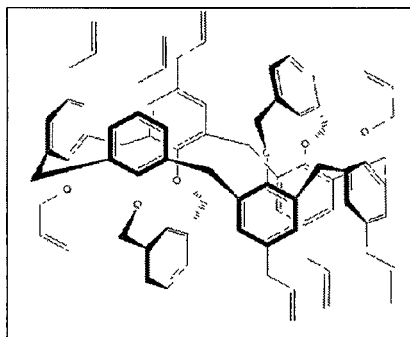
Figure 4.7: Benzene Absorbance Spectrum<sup>12</sup>.

The C=C aromatic stretch band should occur at about 1500 . The absorption spectra should show a sharp absorption at about 1500 . Benzene is highly transparent to the IR, as seen in 4.6, with the only other absorptions in the region under study are two CH bends at 1000 and 675 . There is some evidence of CH bending in each of the spectra, with the more noticeable being the CH bend at around 675 , however, noting the same absorption in Figure 4.6 shows the levels of absorptions are not equal in magnitude. One,

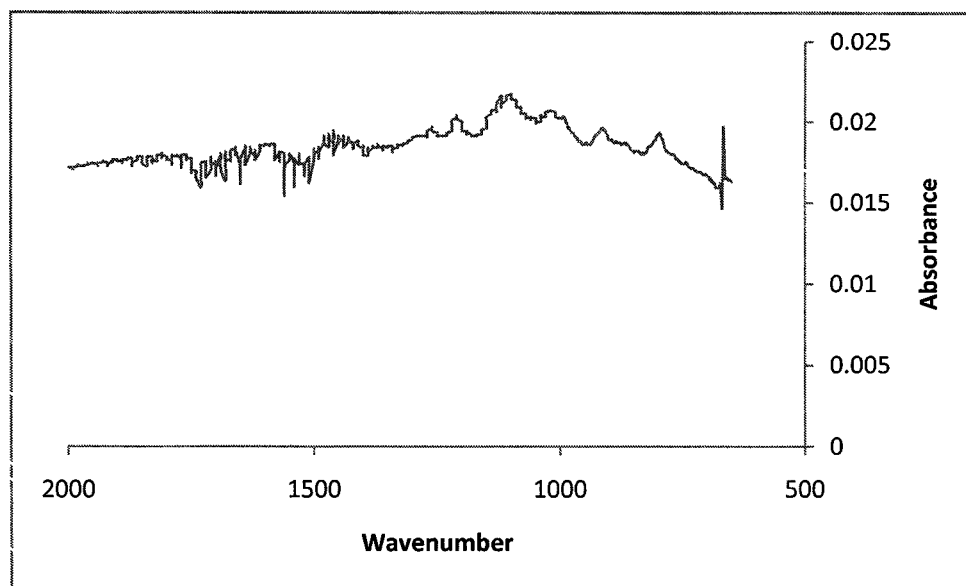
Figure 4.6, shows a totally absorbing peak whereas Spectra 4.1 - 4.6 show only a tiny absorption. This could mean that the amount of calix[6]arene present limits the absorption.

The dramatic change between the 20 minute exposure and the 1000 minute exposure indicates that the exposure had an effect on the molecular structure of the calix[6]arene, however due to the lack of the C=C aromatic stretch at 1500 in the previous spectra, concluding that this is a result of polymerization cannot be made definitively.

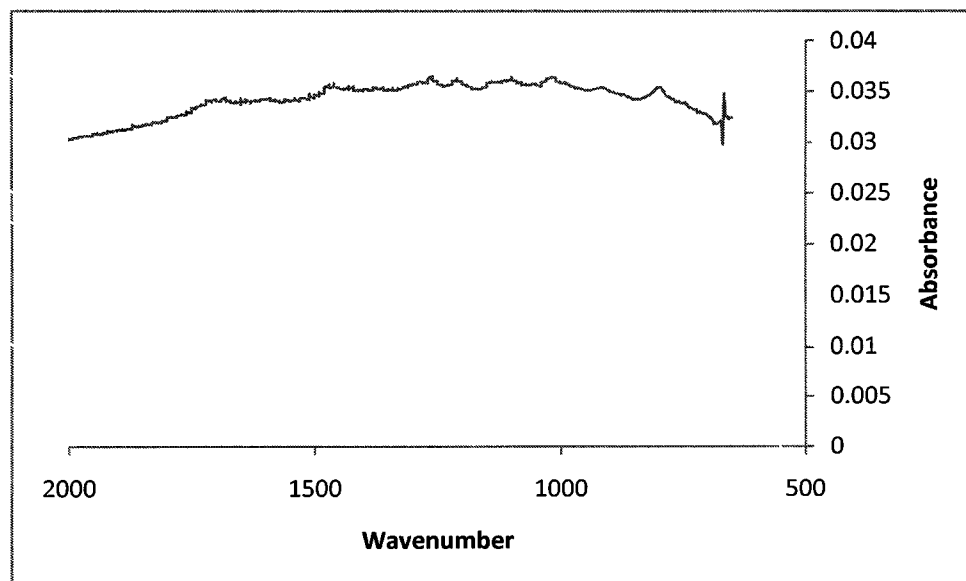
### 8A



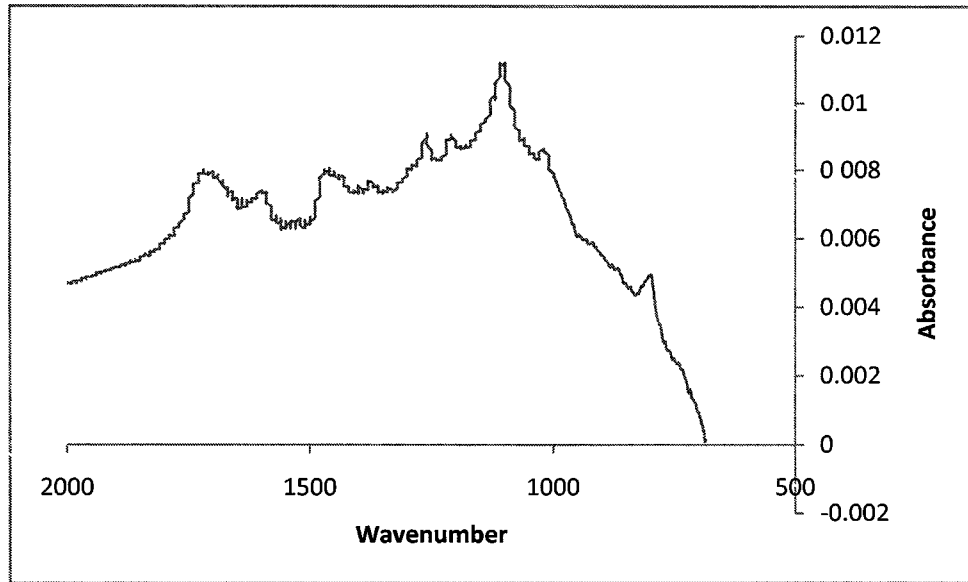
*Spectrum 4.7: Unexposed*



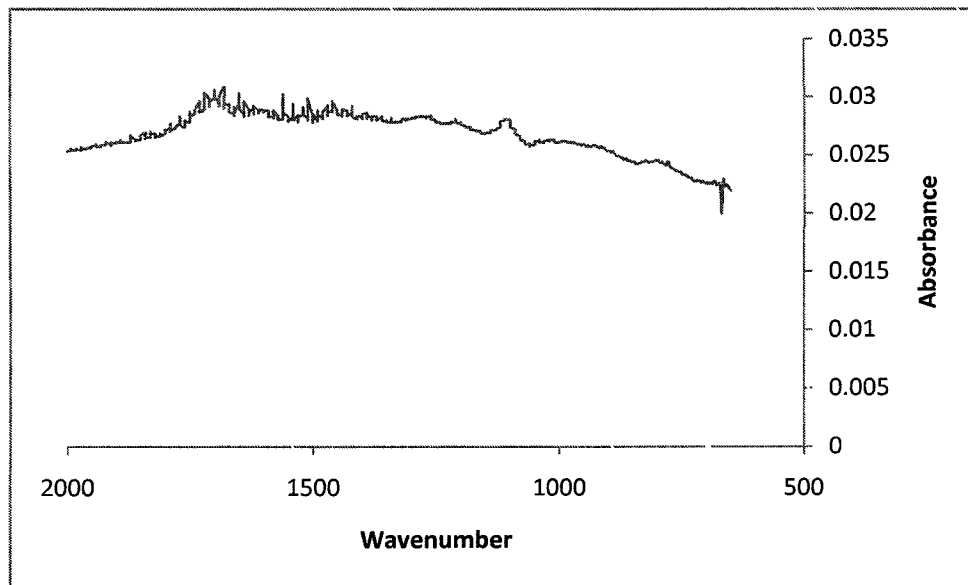
*Spectrum 4.8: 2 minute exposure*



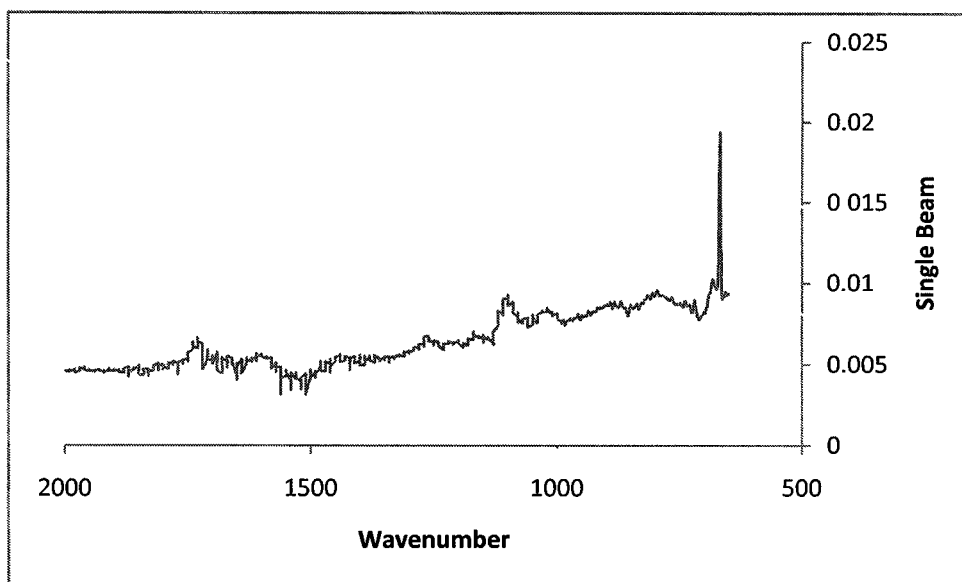
*Spectrum 4.9: 5 minute exposure*



*Spectrum 4.10: 10 minute exposure*



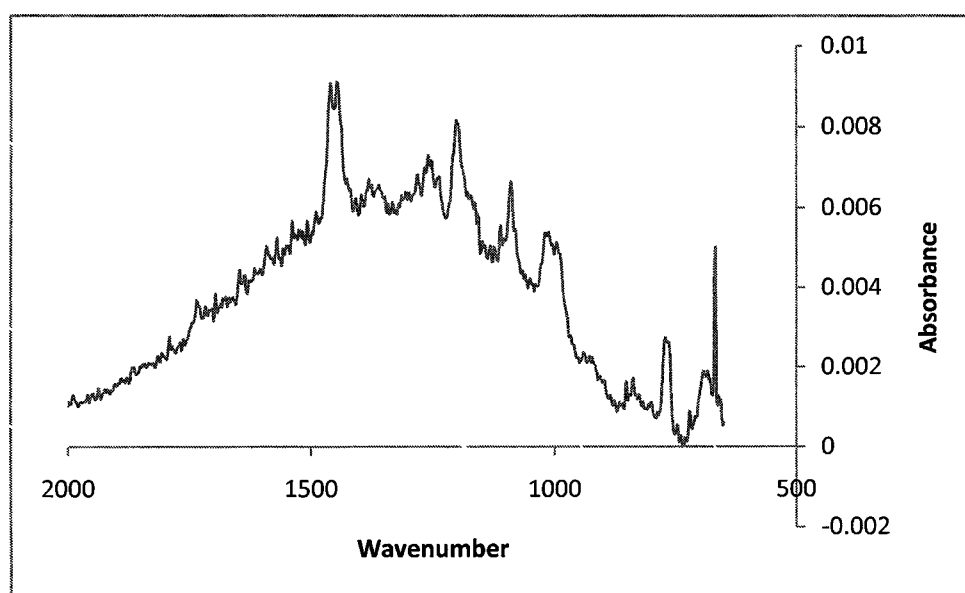
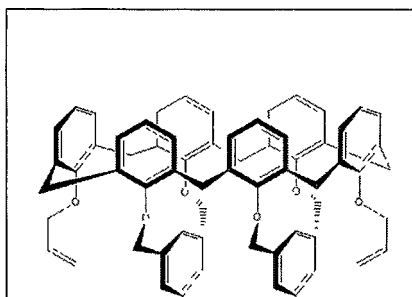
*Spectrum 4.11: 20 minute exposure*



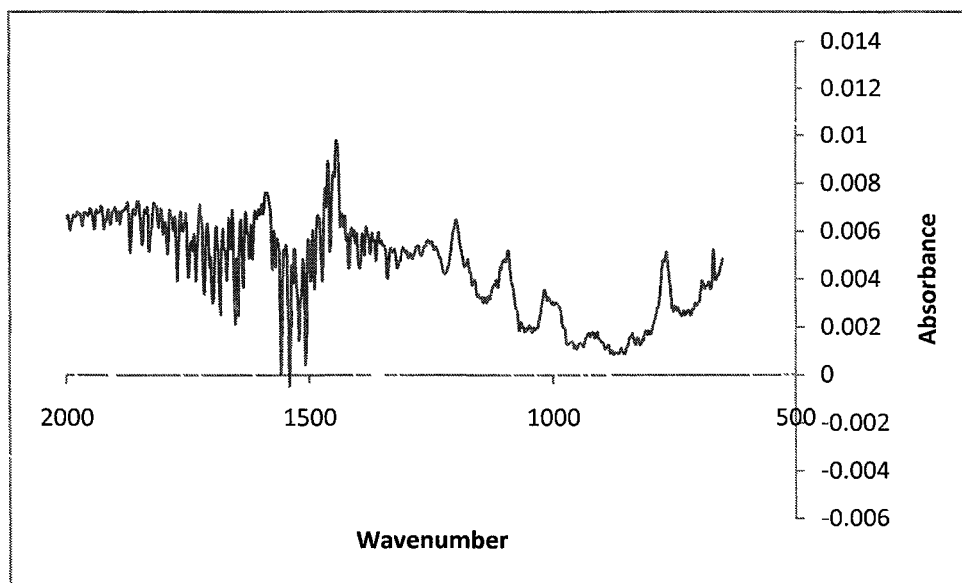
*Spectrum 4.12: 1000 minute exposure*

The absorbance spectra of 8A displayed more IR activity than the 2A species and even showed absorptions in the regions of interest. We can see evidence of C=C stretching at around  $1500\text{ cm}^{-1}$  and C-C stretching around  $1000\text{ cm}^{-1}$ , however the change in the spectra with respect to increased exposure time does not indicate a decrease in the C=C stretch with an increase in the C-C stretch in any spectra except Spectrum 4.10 where there is a significant absorption around  $1000\text{ cm}^{-1}$ . This inconsistency can be attributed to nonhomogeneity of the calix[6]arene film and localization issues. For each successive measurement, the region of the sample measured changed due to removing the sample from the cardboard sample mount for exposure purposes. When placing the sample back onto the mount, it was unlikely that the IR beam intersected the sample in the same region as the previous measurements. These sporadic results do not lend themselves to confirmation of polymerization of the 8A calix[6]arene.

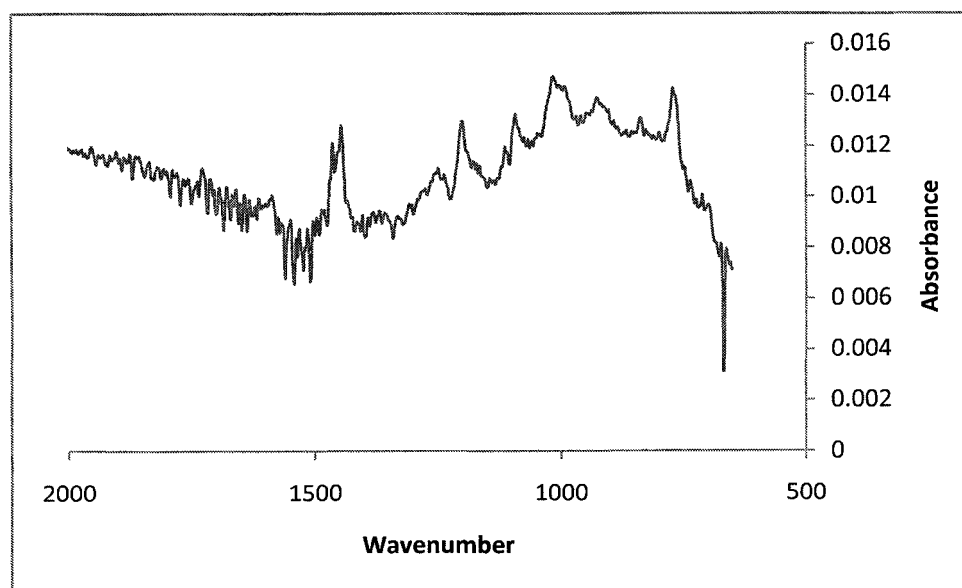
2C



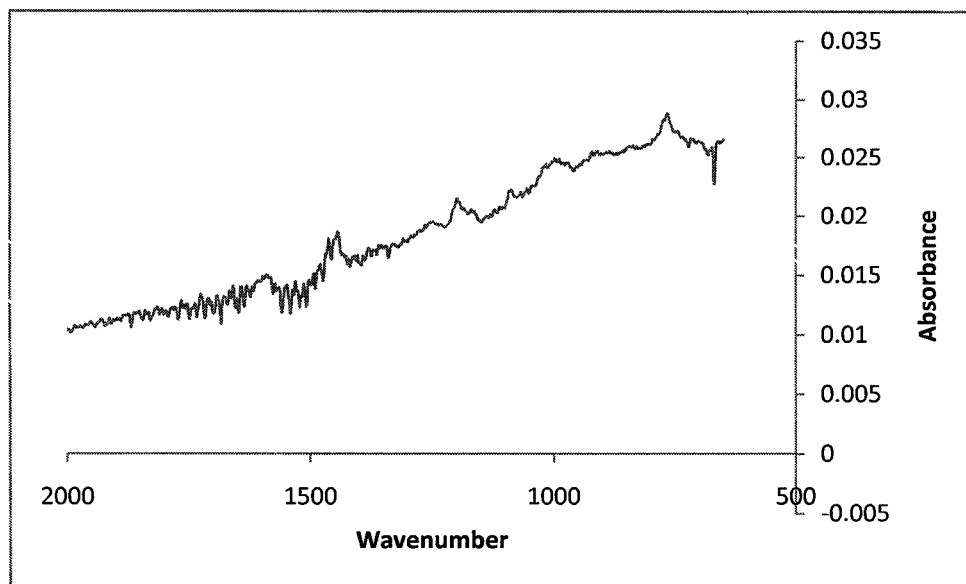
*Spectrum 4.13: Unexposed*



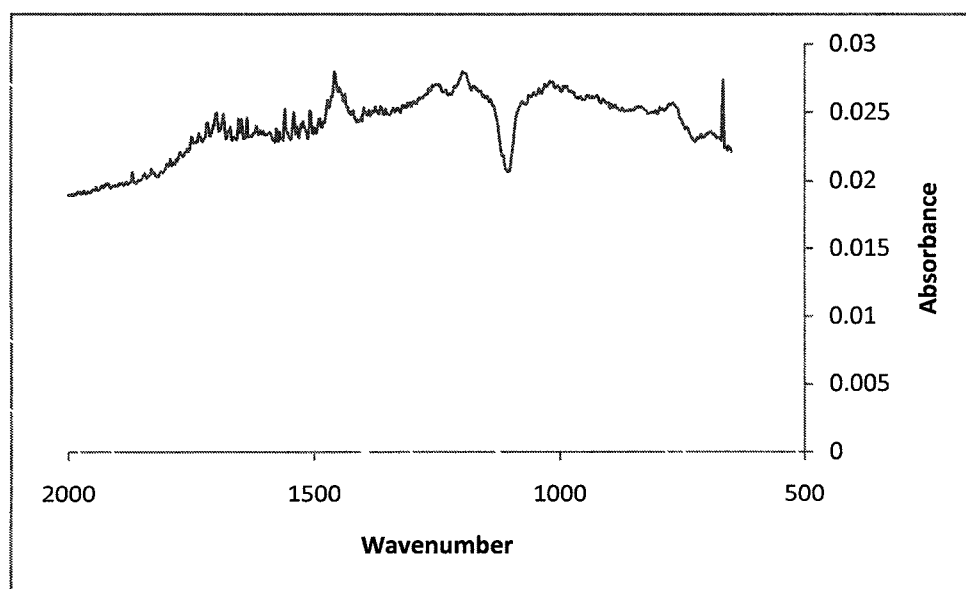
*Spectrum 4.14: 2 minute exposure*



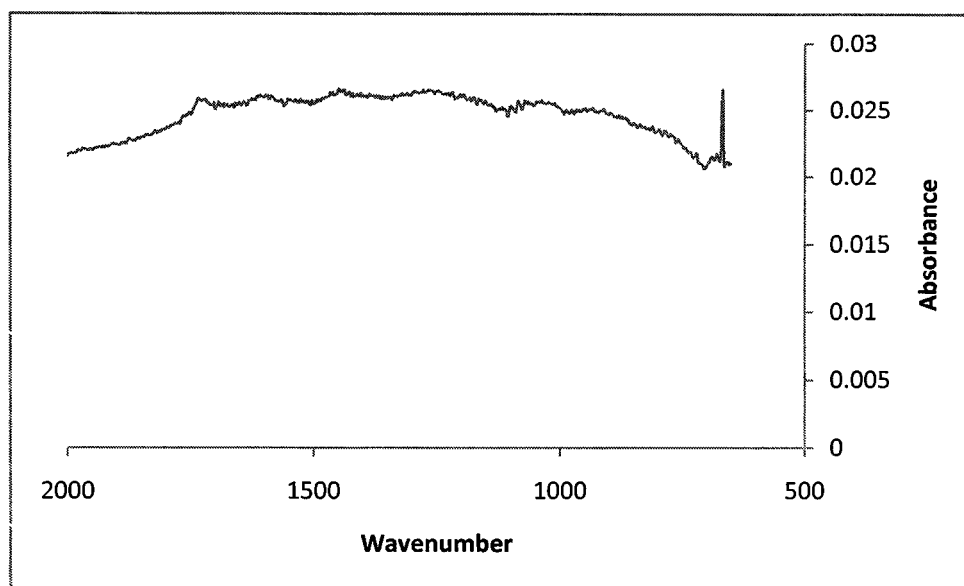
*Spectrum 4.15: 5 minute exposure*



*Spectrum 4.16: 10 minute exposure*



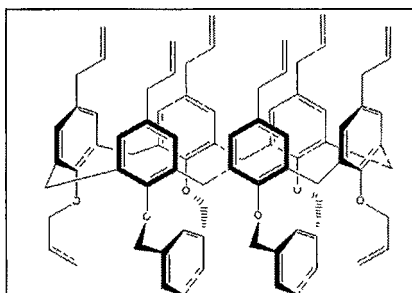
*Spectrum 4.17: 20 minute exposure*

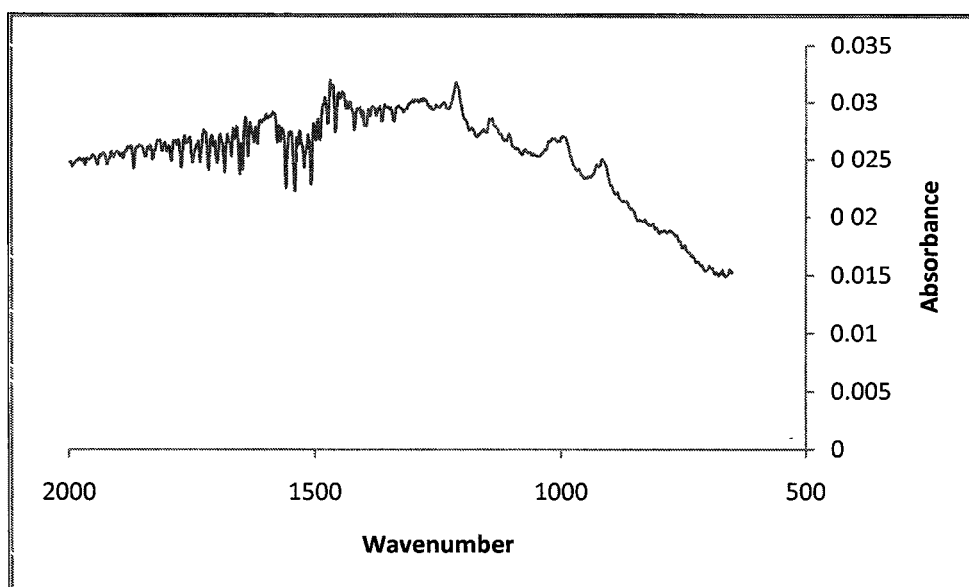


*Spectrum 4.18: 1000 minute exposure*

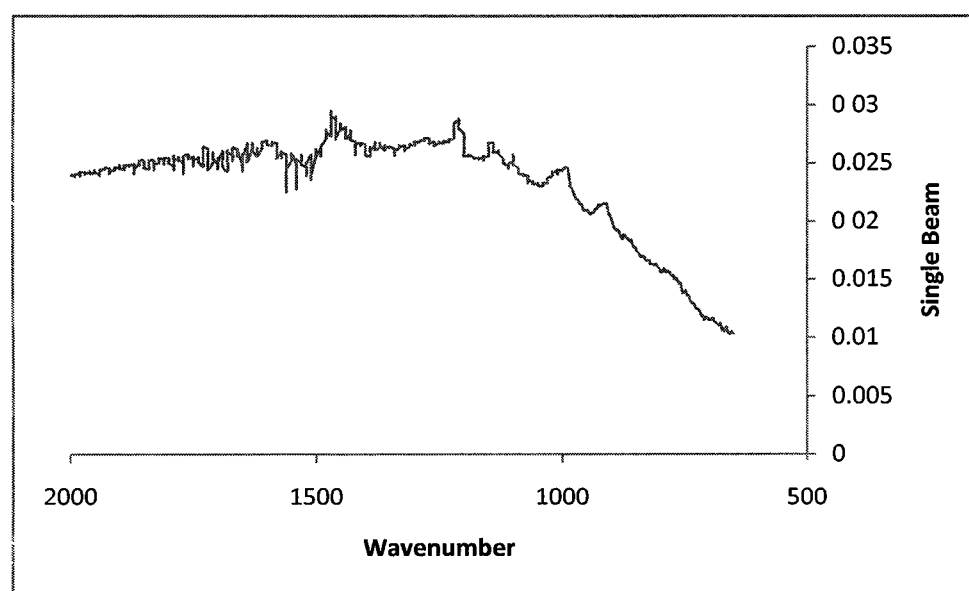
The 2C spectra revealed little information with respect to polymerization. Many of the spectra contained excess absorptions from water which cover the region where a C=C stretch occurs and the spectra showed no continuity with respect to molecular structure. There is no basis for concluding polymerization occurred in the 2C species due to UV exposure.

## 8C

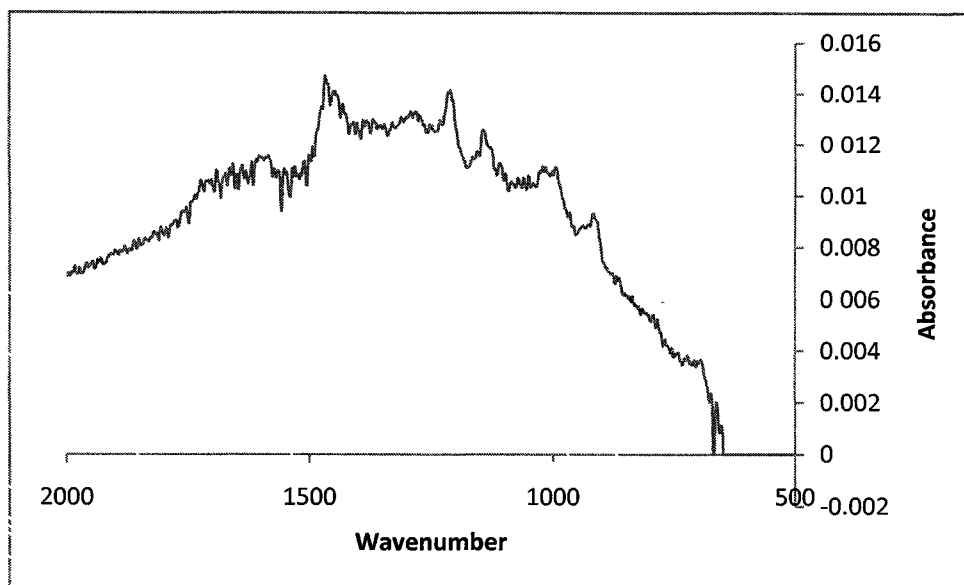




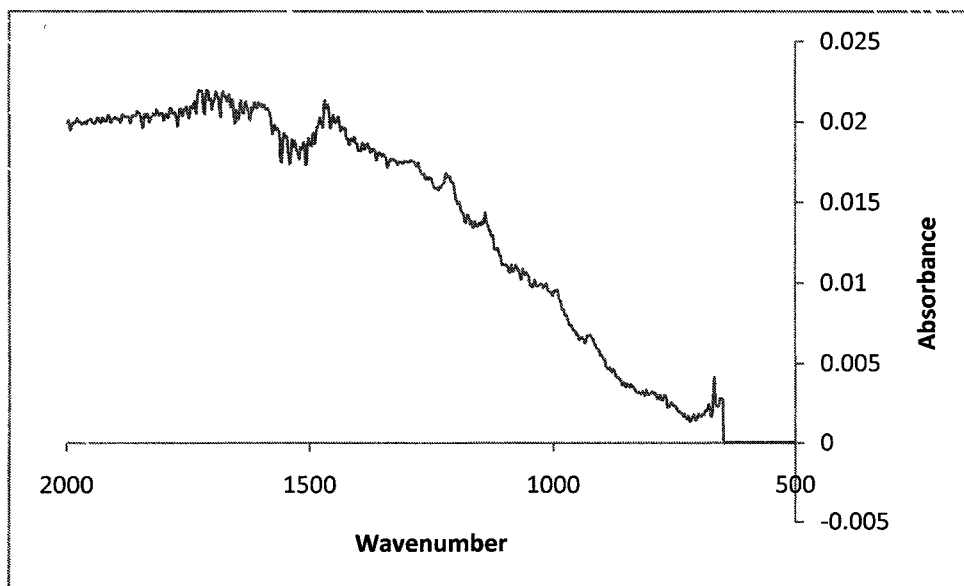
*Spectrum 4.19: Unexposed*



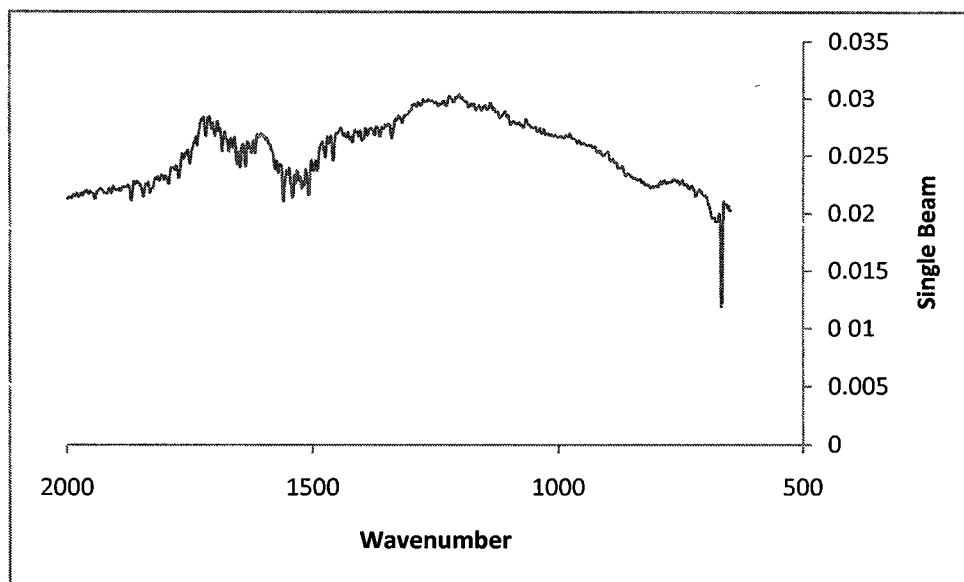
*Spectrum 4.20: 2 minute exposure*



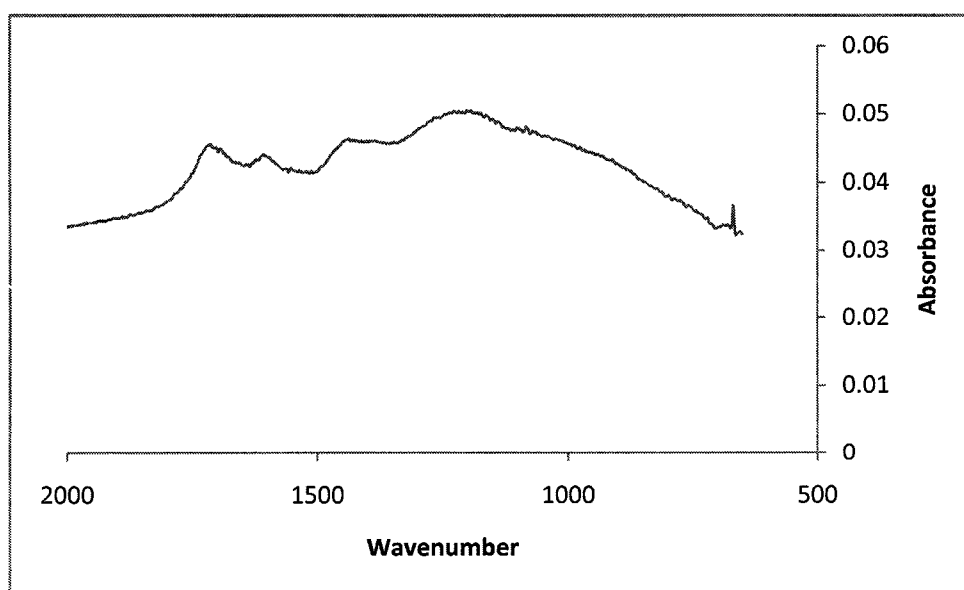
*Spectrum 4.21: 5 minute exposure*



*Spectrum 4.22: 10 minute exposure*



*Spectrum 4.23: 20 minute exposure*

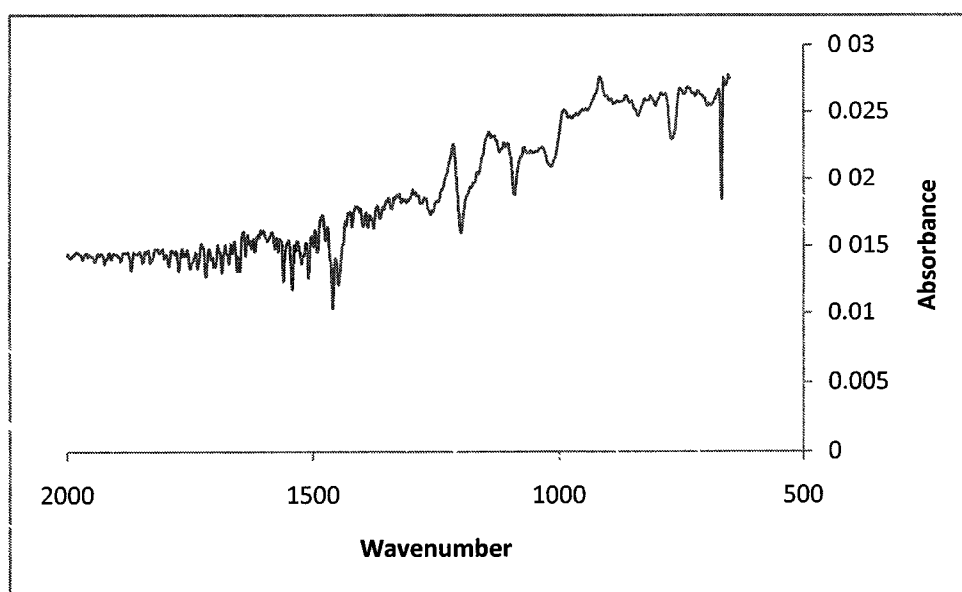


*Spectrum 4.24: 1000 minute exposure*

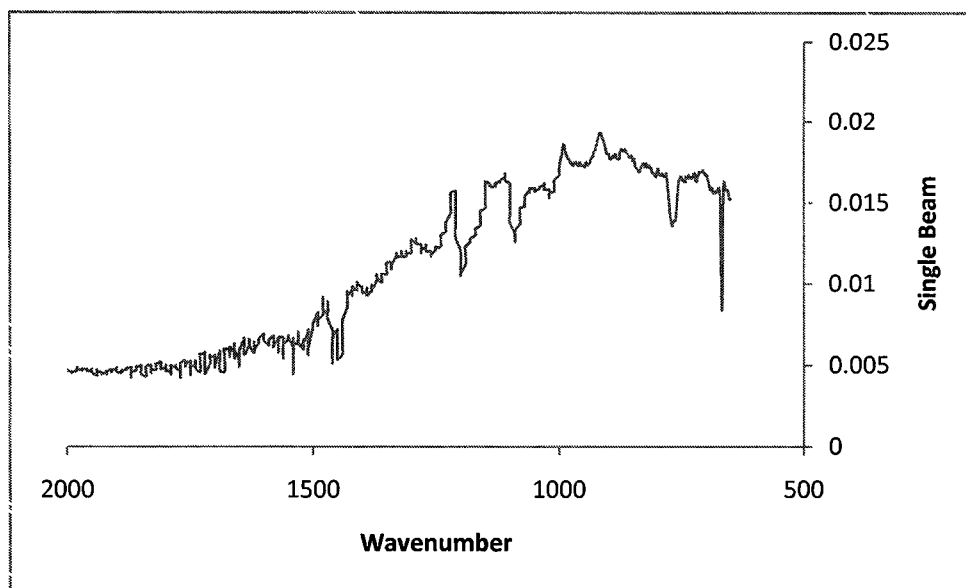
8C did not show evidence of polymerization, however there was evidence of C=C and C-C stretching. The spectra indicate an increase in C=C stretching with

respect to exposure time. This result was unexpected considering they would be broken if polymerized. There is also evidence of an increase in the C-C region around  $1100\text{ cm}^{-1}$  with respect to increased exposure time, which could coincide with polymerization, but making this determination, considering the sporadic results of the previous species limits the ability to be certain this is the case. That topped with the many bonds present in the calix[6]arene, and the fact that the region being studied is in the fingerprint region where all molecules absorb, makes this conclusion even more difficult. The next section looks at the 8C calix[6]arene spectra from a different point of view. In the previous experiments, the background was recorded with silicon included in the background. For the next experiment, silicon with the OC species deposited on it was used in the background spectra. Doing so, in theory will give a spectrum of the attached allyl group only, where the presence of C=C and C-C may be more prominent.

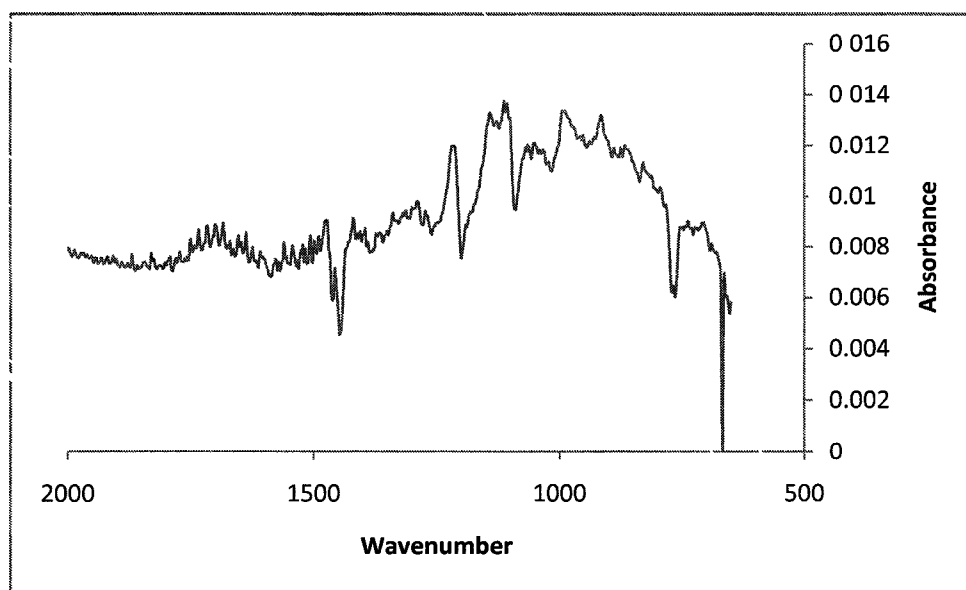
### 8C with Si and OC as the Background



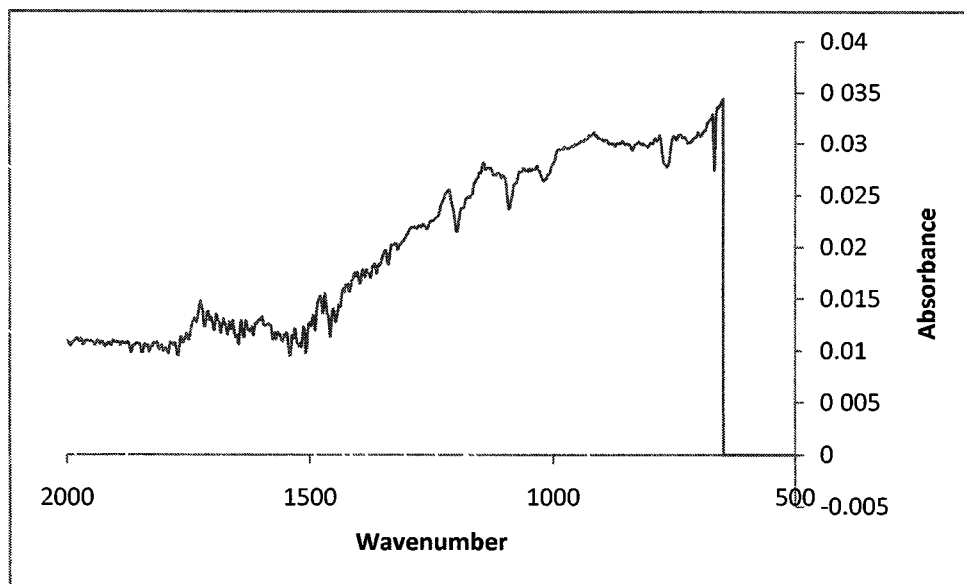
*Spectrum 4.25: Unexposed*



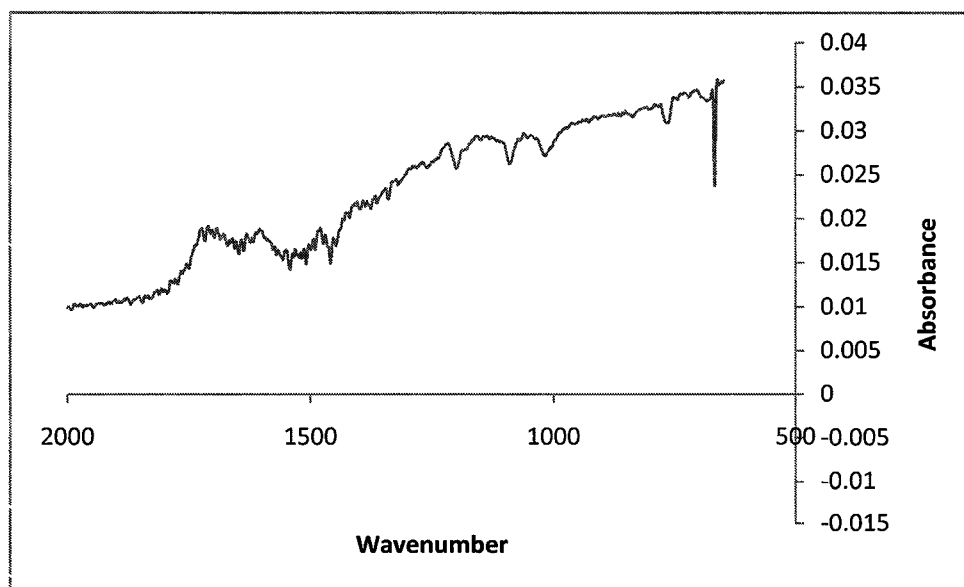
*Spectrum 4.25: 2 minute exposure*



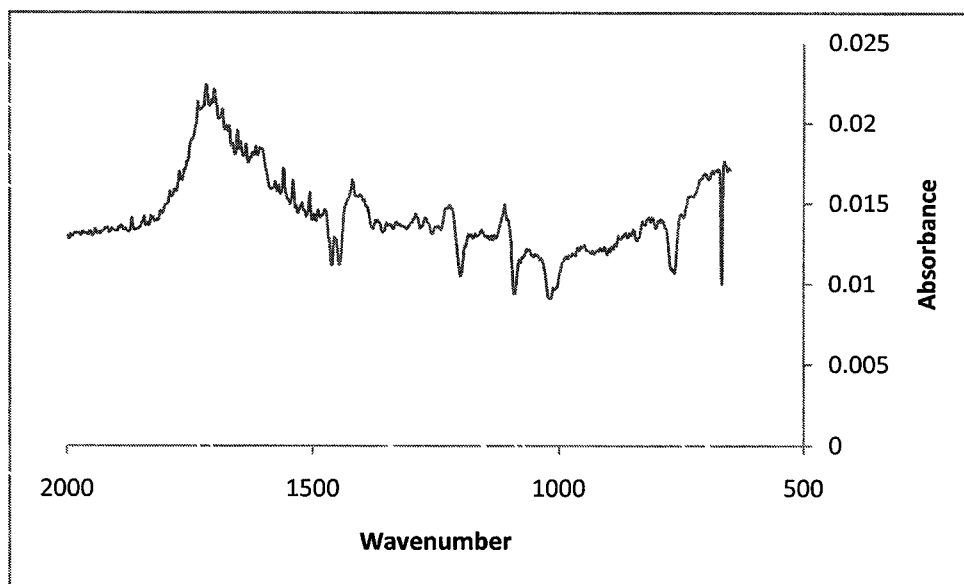
*Spectrum 4.26: 5 minute exposure*



*Spectrum 4.27: 10 minute exposure*



*Spectrum 4.28: 20 minute exposure*



*Spectrum 4.30: 1000 minute exposure*

Using this method revealed a true pattern, showing an increased absorption of the C=C stretch with increased exposure time. The unexposed spectra shows a broad absorption

From  $675\text{ cm}^{-1}$  to just below  $1500\text{ cm}^{-1}$  which is due to the multiple absorptions present in that region. As exposure time increased, absorptions in this region decrease and become overtaken by the C=C stretch absorption which coincides with the results obtained using only silicon in the background. These results, however, do not coincide with the expected results. In fact they are just the opposite. This could suggest that polymerization has occurred, but the polymerization occurs differently than previously thought. Or it could suggest that the effect of UV exposure of calix[6]arenes does not cause polymerization of the calix[6]arene. Detection of polymerization of the calix[6]arenes using FTIR was inconclusive.

## CHAPTER 5

### CONCLUSION

The results of the experiments did not show clear evidence of polymerization and in the case of the 8C calix[6]arene, even displayed results countering what was originally expected. These results do not discount using FTIR as a polymerization detection technique, but do shed light concerning the methodology at each step of the process. There are process steps at each interval which can be improved upon. Below are improvements listed which I believe would improve the experiment and yield better films and spectra.

The wafer spinner settings used (3000 rpm for 30 sec) spun on very thin films. This was evident in the minimal absorption levels. By decreasing the rpm setting, thicker films could be produced. Thicker films will exhibit higher absorption levels and leave more calixa[6]arenes to be polymerized per sample. A study of absorption vs film thickness could maximize the level of absorption and provide a better benchmark for film thickness for this purpose.

The UV lamp used for exposure was a broadband UV source. There is little certainty about how this affected the calix[6]arene. UV radiation is able to break molecular bonds and since the source contains a broad spectrum of energy, other bonds may have been broken than just the C=C bond. To remedy

this, use of a laser tuned to the energy to break a double carbon bond specifically could provide a better exposure technique. The double carbon bond has a sigma bond and a pi bond with the pi bond being the more reactive of the two. The bond energy of the double carbon bond is approximately 6.29 eV or 197 nm, however this is the total energy. If we consider the energy of a single carbon bond is about 3.5 eV and subtract that from the 6.29 eV we are left with 2.79 eV. This means that the two bonds have different dissociation energies. A laser tuned to break the lesser of the two bonds could be more sufficient for this experiment. A 444 - 445 nm laser could be used to break the 2.79 eV bond.

The spectra taken revealed many inconsistencies due to localization issues. From one spectrum taken to the next, the sample was not mounted in exactly the same position as the previous measurement, which led to sporadic results. Care was taken to prevent this however the cardboard mount used only two-sided tape to hold the sample in place. Many times the sample fell off the mount and required replacement. This is also an issue of film homogeneity mentioned previously as different areas of the sample had different amounts of calix[6]arene present.

The calix[6]arenes are designed to be exposed by an electron beam source. Using an SEM (Scanning Electron Microscope) as the electron beam source has been used and shown to polymerize the calix[6]arene, however due to the sizes of the areas exposed (~ 20 microns), taking FTIR spectra of these samples using the transmission technique used would be a daunting task. Lining up the IR beam with such a small area would not be an easy task. Using a FTIR microscope could provide a method to do so. Also, larger areas can be exposed

using the SEM, but for use with the FTIR, a sample would have to be exposed for a long period of time. A  $20 \mu m^2$  sample requires approximately 20 minutes to be exposed. Increasing the exposure size also requires more time to expose the sample. To make a sample of approximately  $5 mm^2$ , an ideal size for the FTIR transmission technique, would require up to 1000 minutes to ensure the whole region was exposed in the same manner as the  $20 \mu m^2$  sample. Using the FTIR microscope would negate the need for 1000 min exposures and would also ease the problems of localization encountered by the method used in this study.

## **Appendix**

### **Nicolet 6700 Series FTIR Operation and OMNIC Computer Interface <sup>13</sup>**

The Nicolet 6700 series FTIR spectrometer allows collection of spectra in the near-IR, mid-IR and far-IR. All settings can be adjusted using the computer interface called OMNIC. These settings include, but are not limited to choosing the detector type, beam-splitter, light source, spectral range, spectra measurement type (absorbance, transmittance, reflectance, etc.), resolution, number of scans, aperture, and gain. These are the basic elements of the Nicolet FTIR spectrometer and understanding these elements greatly increases the ability to collect reliable spectra.

#### **Purging and Desiccating the Spectrometer**

The first step in using many spectrometers is purging the system. This is done using a non-flammable gas, usually Nitrogen, and requires a minimum of two hours to be done efficiently. Purging the spectrometer removes many excess gasses and particulates from the air surrounding the internal components of the spectrometer and greatly increases spectral quality. Anything in the path of the light source en route to the sample will absorb energy and saturate the spectra with extra peaks, which can be deceiving when interpreting the spectra. Nitrogen is used as a purge because it is highly transparent to infrared and visible light.

Nitrogen is a homonuclear molecule, having no dipole moment to couple to electromagnetic radiation at these wavelengths so saturating the spectrometer with Nitrogen will add few if no peaks in the resulting spectra. The Nicolet spectrometer requires between 20 psi and 40 psi of pressure and can be adjusted manually using a pressure gauge located on the gas valve of the Nitrogen dewar. A typical pressure is 25 psi.

A chemical agent is used to desiccate the spectrometer. The desiccant removes moisture from the air in the sealed compartment of the spectrometer. Water can be damaging to the optical components of the spectrometer (beamsplitter, lenses, mirrors). The only task here is to routinely check the desiccant ensuring the agent is still efficiently removing moisture from the air. This can be done in two ways. The desiccant is located underneath the beamsplitter compartment cover and has an indicator tab that is blue if desiccant is acceptable, pink if unacceptable. One can also check the status of the desiccant more accurately using the check desiccant button located under the diagnostics tab, which is found under the experiment setup tab. This is the recommended method to check the desiccant while the spectrometer is in use since it is more accurate.

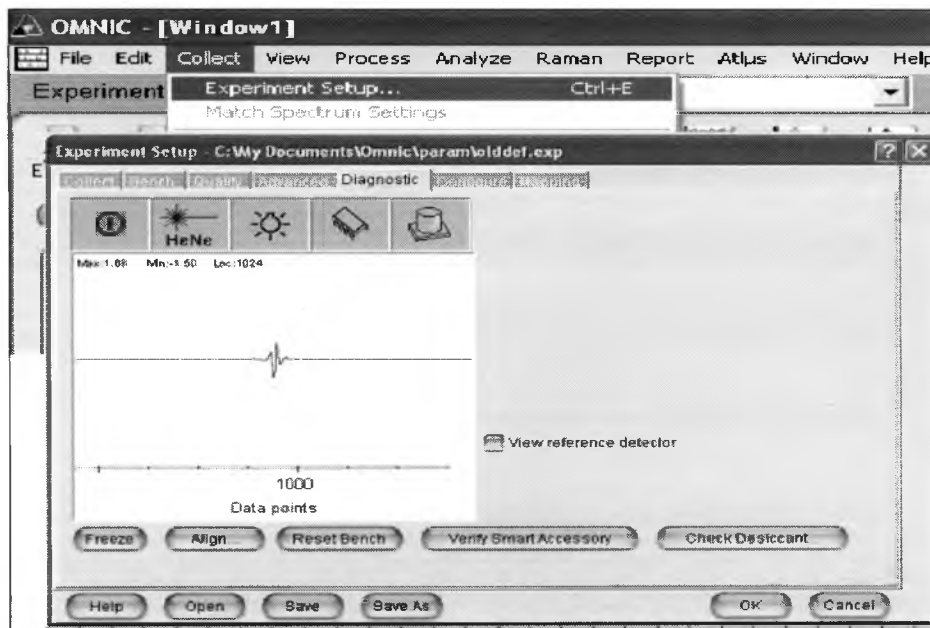


*Figure A.1. Checking the Dessiccant. Needs routine checking to ensure safety of all internal components.*

### Setting up an Experiment.

Depending on the type of data desired, different steps must be taken to ensure quality spectra. For any spectra, sample preparation is a vital part of ensuring good spectral quality. Avoid touching samples with bare hands as oils and other particulates can contaminate a sample. Isopropanol (Isopropyl alcohol) works well in dissolving oils and can be used to clean many solids and thin films. If a sample is dirty, clean it with a swab soaked in Isopropanol and ensure it is dry before taking any measurements. Contaminated liquid samples should be dispelled and a new sample should be prepared. Once the sample is prepared, one can begin setting up the experimental parameters. All of the parameters can be set in the experiment setup window shown below in Figure A.2.

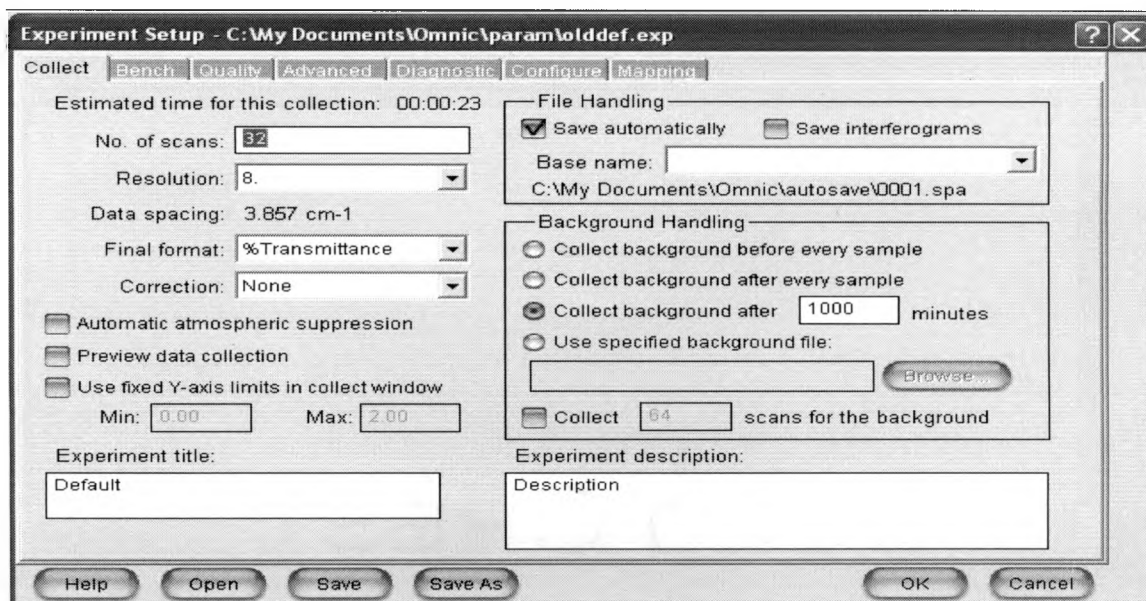


*Figure A.2. Experiment Setup Window - Collect tab. Used for choosing the type of experiment (absorbance, transmittance, reflectivity..etc.), scan resolution and number of scans per spectra as well as background handling.*

**Number of scans:** Choosing the number of scans for an experiment is important because the more scans taken for a given spectra, the better the signal to noise ratio is resulting in a more comprehensible spectra.

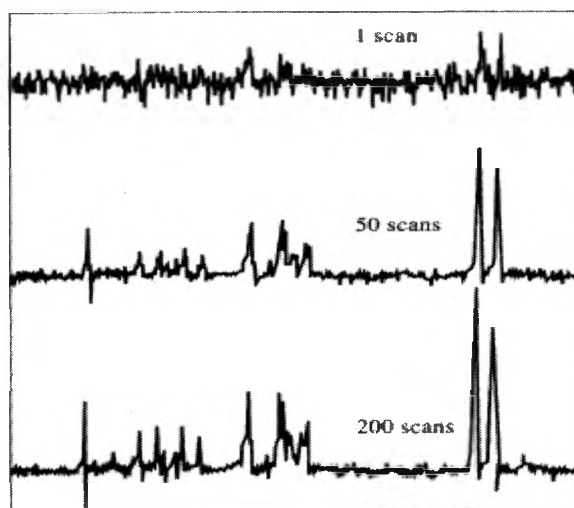


*Figure A.3: Signal to Noise Improvement. The more scans taken improves the S/N ratio but increases the amount of time necessary to record a spectrum.*

**Resolution:** The resolution of the spectrum describes the distance between data points recorded in the spectrum and is proportional to the distance the movable mirror travels per scan. Smaller resolution values result in more accurate spectra, however some resolutions may be too small for a specific experiment due to the availability of the experimental setup desired. For example, sometimes the aperture setting, which will be discussed later, is too large to achieve smaller resolutions. For some experiments, a large aperture is necessary in order to detect a strong enough signal at the detector. In this case, the best possible resolution is the lowest possible resolution possible. The possible values for resolution are 2,4,6,and 8 - 2 being the smallest distance between data points, 8 being the largest distance.

**Final Format:** The final format of the spectra refers to what kind of measurement you wish to take. Most common formats are absorbance, % reflectance and % transmittance.

**Background Handling:** This describes how and when you collect a background for a spectra or if you wish to revert to a saved background spectrum. Background spectra are necessary because they record the spectra of anything the source beam interacts with along its path through the spectrometer. Once a background spectrum is recorded, it can be subtracted from the sample spectrum, leaving only the spectrum of the sample being studied. Background files can be saved for use at a later time. This is especially useful when performing low temperature measurements requiring a lot of time to setup.

**Detector/Beamsplitter Combinations:** The next step in experiment setup involves choosing the combination of beamsplitter and detector you wish to use. This requires a clear understanding of the materials being measured as well as the energy ranges you want to evaluate. Some detectors are better for some ranges than others and the same can be said for beamsplitters. The idea is optimizing the combinations to receive the highest quality spectra possible. Combinations are considered compatible if they provide a detector signal large enough to allow beamsplitter alignment. Figure A.4 lists the possible combinations and rates them as incompatible (X), compatible (OK), or optimum (Best).

DETECTOR	BEAMSPLITTER					
	Near-IR			Mid-IR*		Far-IR
	Quartz	CaF <sub>2</sub>	XI-KBr	KBr	Cl	Solid Substrate
DTGS (KBr window)**	X	OK	Best	Best	OK	X
DTGS (Cl window)	X	X	OK	OK	Best	X
DTGS (PE window)	X	X	X	X	OK	Best
MCT-A	OK	OK	Best	Best	OK	X
MCT-B	OK	OK	Best	Best	OK	X
InSb	OK	Best	OK	X	X	X
PbSe	OK	Best	OK	X	X	X
Si	Best	OK	X	X	X	X
PbS	OK	Best	X	X	X	X
InGaAs	OK	Best	OK	X	X	X

Best= Optimum beamsplitter-detector combination.  
 OK= Compatible beamsplitter-detector combination.  
 X= Incompatible beamsplitter-detector combination

*Figure A.4: Optimal Beamsplitter-Detector Combinations<sup>11</sup>.*

The Nicolet 6700 series FTIR spectrometer has two detector types - MCT/A and DTGS. The MCT/A (mercury cadmium telluride) detector is a liquid nitrogen cooled detector and operates the best with a KBr beamsplitter in the near and mid IR range however it is not compatible with the far IR range. The /A

represents the type of screen used on the detector and limits the amount of light incident on the detector, preventing detector saturation. Figure A.5 shows the screens available and the amount of light transmitted to the detector.

Screen	% Transmitted*	Detectors Typically Used With Screen
None	100	DTGS, MCT-B
A	30	MCT-A
B	10	PbSe, InSb
C	3	
D	1	

*Figure A.5: Screen Type Versus Transmitted Radiation.*

An advantage of the MCT detector is the improvement of signal to noise ratio compared to other detectors. For a given scanning time, an MCT detector will produce a spectrum with a noise level 10 to 100 times lower than the noise from a DTGS detector. This limits the amount of scans necessary for quality spectra which reduces the amount of time needed to record the spectra. The DTGS (deuterated triglycine sulfate) detector records more noise than the MCT, however for many solids and liquids, it will be sufficient. It is also compatible with the far IR where the MCT is not compatible. To select a beamsplitter/detector, open the Bench tab under Experiment Setup. See Figure A.6. Note\* Choosing a new detector or beamsplitter automatically resets the recommended (default) range in the Experiment Setup window. These ranges can be adjusted, however, The regions of the spectra outside of the recommended range will be of lower quality.

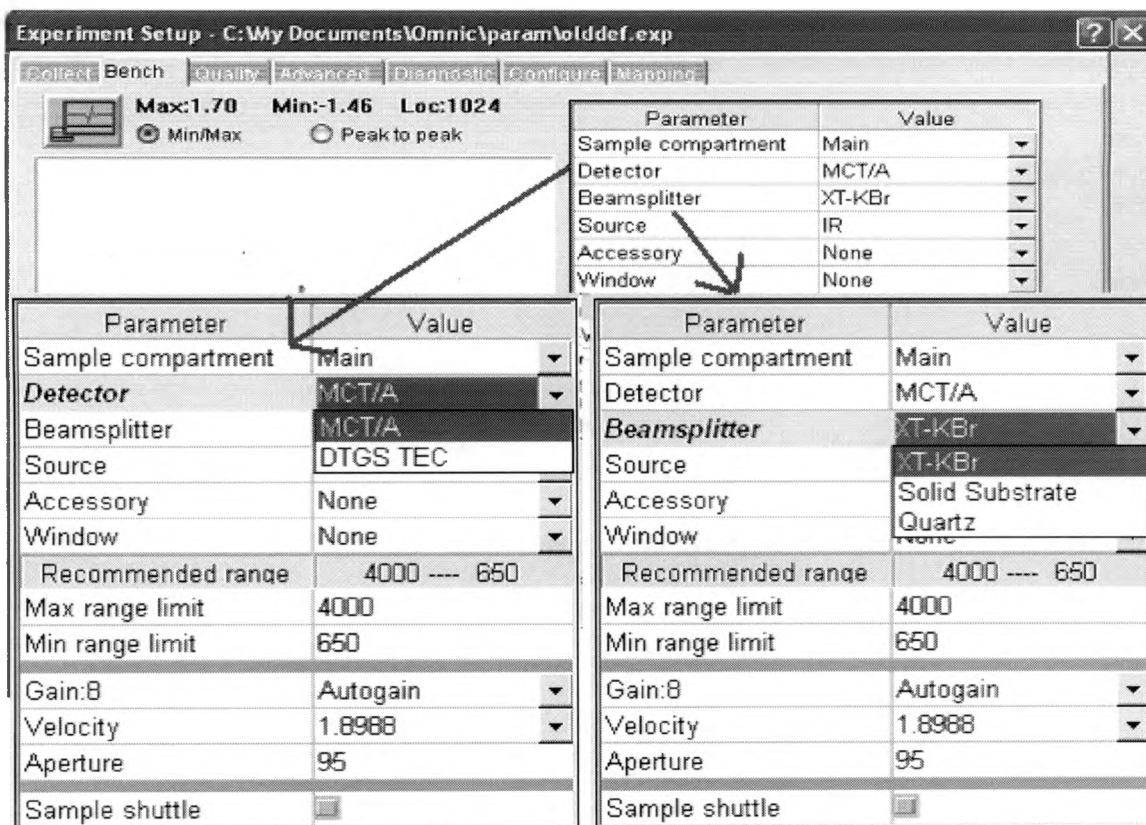


Figure A.6: Bench Tab of Experiment Setup Tab.

**Source:** Choosing a source depends on what spectral range you wish to measure. The Nicolet spectrometer is equipped with two sources, one being an Everglow source used for the mid and far IR, and a white light source for the near IR range.

**Gain:** Amplifies the detector signal intensity making it larger with respect to noise. OMNIC will automatically adjust the gain to maximize the signal by setting the Gain to Autogain, ensuring the best spectral quality possible

**Velocity (Mirror).** Increases/decreases the velocity at which the moving mirror scans in cm/s. Increasing mirror velocities limits resolution as velocity increases. Typically mirror velocities are increased to decrease scan time, however, unless hundreds of scans are being taken, increasing mirror velocity is unnecessary.

**Aperture:** The aperture in the Nicolet 6700 spectrometer is a variable diameter opening controlling the angular size of the beam, thus controlling the amount of radiation transmitted to the sample. Apertures allow the use of more sensitive detectors (MCT), prevent IR saturation at the detector, and acts as a point source, improving resolution and wavenumber accuracy. Larger aperture settings increase the signal to noise ratio while small aperture settings are key to high-resolution settings. Recommended settings for the different detectors are as follows: DTGS -100; MCT/A - 32. The settings can be adjusted however these values are maximized for optimum detector intensity.

**Accessories:** The Nicolet 6700 series spectrometer is a multifunctional spectrometer compatible with many Smart accessories able to expand the functionality of the spectrometer.

## Bibliography

- <sup>1</sup>Wikipedia, *Moore's Law*, [http://en.wikipedia.org/wiki/Moore's\\_Law](http://en.wikipedia.org/wiki/Moore's_Law)
- <sup>2</sup>International Technology Roadmap for Semiconductors, 2007 Edition, International Sematech, Retrieved March 2008.  
<http://www.itrs.net/Links/2007ITRS/Home2007.htm>
- <sup>3</sup>Kendall, Russel C., *Charaterization of Differentially Functionalized, Conformationally Locked Calix[6]arenes as Negative Electron-Beam Lithography Resist*. Texas State University-San Marcos, May 2007.
- <sup>4</sup>Taylor, Barry N., "The NIST Reference on Constants, Units, and Uncertainty", NIST Physics Laboratory, Version 5.0 Updated 7 March 2007, Retrieved on March 1, 2008,  
<http://physics.nist.gov/constants>.
- <sup>5</sup>Manako, Shoko.; Ochiai, Yokinuri, *High-Purity, Ultrahigh-resolution calixarene electron-beam negative resist*. Journal of Vacuum Science and Technology. B 18(6), Nov/Dec 2000.
- <sup>6</sup>Monreal, Gabriel H.; Staggs, Sara J.; Blanda, Micheal T.; Geerts, Wilhelmus J.; Galloway, Heather C.; Spencer, Gregory C. *Synthesis, characterization, and investigation of a conformationally immobile calix[6]arene as a negative electron beam resist*. Department of Chemistry/Physics, Texas State University. Published Online -14 September 2005. Retrieved March 28,2008.  
<http://scitation.aip.org/getabs/servlet/GetabsServlet?prog=normal&id=JVTBD9000023000005001998000001&idtype=cvips&gifs=yes>
- <sup>7</sup>Infrared Spectroscopy. Retrieved on February 28, 2008. Information on webpage adapted from R. L. Pecsok L. D. Shields, *Modern Methods of Chemical Analysis* (Wiley, New York, 1968);and A.T. *Chemical Analysis* (Wiley, New York, 1968); and A.T.

Schwartz et al., *Chemistry in Context* (American Chemical Society, Washington, DC 1994).  
<http://www.wag.caltech.edu/home/jang/genchem/infrared.htm>

- <sup>8</sup>Nature of Vibrational Spectroscopy. Retrieved on March 10, 2008.  
<http://www.cem.msu.edu/~reusch/VirtualText/Spectrpy/InfraRed/.htm#ir1>
- <sup>9</sup>Halliday, David; Resnick, Robert; Walker, Jearl. *Fundamentals of Physics*. Sixth Edition John Wiley & Sons, New York 2001.
- <sup>10</sup>Griffiths, Peter R.; de Haseth, James A., *Fourier Transform Infrared Spectroscopy*, Wiley Interscience: New York, 1986
- <sup>11</sup>Smith, Brian C. *Fundamentals of Fourier Transform Infrared Spectroscopy*. Retrieved on February 28, 2008.  
[http://books.google.com/books?id=cL\\_cvNCoEmkC&dq=fundamentals+of+fourier+transform+infrared+spectroscopy&pg=PP1&ots=l5YNg-m3cb&sig=QNQ8hrdkh0XSc6C3ILfWzndNc&hl=en&prev=http://www.google.com/search?hl=en&sa=X&oi=spell&resnum=0&ct=result&cd=1&q=fundamentals+of+Fourier+Transform+infraredy&spell=1&oi=&ct=title&cad=one-book-with-thumbnail#PPP1,M1](http://books.google.com/books?id=cL_cvNCoEmkC&dq=fundamentals+of+fourier+transform+infrared+spectroscopy&pg=PP1&ots=l5YNg-m3cb&sig=QNQ8hrdkh0XSc6C3ILfWzndNc&hl=en&prev=http://www.google.com/search?hl=en&sa=X&oi=spell&resnum=0&ct=result&cd=1&q=fundamentals+of+Fourier+Transform+infraredy&spell=1&oi=&ct=title&cad=one-book-with-thumbnail#PPP1,M1)
- <sup>12</sup>Essential FTIR v1.20 build 137 Full Featured Trial Version. BENZENE FDM FTIR Spectra of Organic Compounds. Fiveash Data Management Inc. 1997.
- <sup>13</sup>Thermo Electron Corporation. *Nicolet<sup>tm</sup> FT-IR Users Guide*.

## VITA

Matthew Josiah McDougle was born in New Branfels, Texas, on January 7, 1979, the son of Suzanne McDougle and Donald Bryant McDougle. Upon Graduating from Samuel Clemens High School in 1997, he joined the Navy where he served his country for four years. Upon completion of Navy service, Matthew enrolled at Texas State University-San Marcos. He received his bachelors degree in Physics in May 2005. The following Fall he began his graduates studies in physics at Texas State and in May 2008, he received a Master of Science in Physics.

Permanent Address:       N/A

This thesis was typed by Matthew Josiah McDougle